J Comput Neurosci (2006) 21:307–328
DOI 10.1007/s10827-006-8862-7

Differential control of active and silent phases in relaxation models of neuronal rhythms

Joël Tabak · Michael J. O'Donovan · John Rinzel

Received: 21 March 2005 / Revised: 16 March 2006 / Accepted: 18 April 2006 / Published online: 28 July 2006

Abstract Rhythmic bursting activity, found in many biological systems, serves a variety of important functions. Such activity is composed of episodes, or bursts (the active phase, AP) that are separated by quiescent periods (the silent phase, SP). Here, we use mean field, firing rate models of excitatory neural network activity to study how AP and SP durations depend on two critical network parameters that control network connectivity and cellular excitability. In these models, the AP and SP correspond to the network's underlying bistability on a fast time scale due to rapid recurrent excitatory connectivity. Activity switches between the AP and SP because of two types of slow negative feedback: synaptic depression—which has a divisive effect on the network input/output function, or cellular adaptation—a subtractive effect on the input/output function. We show that if a model incorporates the divisive process (regardless of the presence of the subtractive process), then increasing cellular excitability will speed up the activity, mostly by decreasing the silent phase. Reciprocally, if the subtractive process is present, increasing the excitatory connectivity will slow down the activity, mostly by lengthening the active phase. We also show that the model incorporating both slow processes is less sensitive to parameter variations than the models with only one process. Finally, we note that these network models are formally analogous to a type of cellular pacemaker and thus similar results apply to these cellular pacemakers.

Keywords Excitatory network · Synaptic depression · Cellular adaptation · Episodic activity · Mean field model

Action Editor: Misha Tsodyks

J. Tabak · M. J. O'Donovan
Laboratory of Neural Control, NINDS/NIH,
Bethesda, MD, 20892

J. Rinzel
Center for Neural Science and Courant Institute of Mathematical Sciences, New York University,
NY, 10003

J. Tabak (✉)
Department of Biological Science,
Florida State University,
Tallahassee, FL, 32306-4340
e-mail: joel@neuro.fsu.edu

1. Introduction

Bursts, i.e periodic alternation between periods of activity and periods of quiescence, are generated by a variety of cells and cell assemblies. Cellular pacemakers include secretory cells, respiratory neurons, cardiac cells and invertebrate neurons (Coombes and Bressloff, 2005). Assemblies of such cells give rise to population bursting activity, but network bursting can also occur even if no cell within the network has pacemaker capabilities. For example, developing and disinhibited networks exhibit such episodic activity (O'Donovan, 1999).

These rhythmic activities play essential roles in an organism (control of hormone secretion, respiration, locomotion, etc.) or in the development of neuronal circuits. The characteristics of these activities, for example its period, may be critical in achieving a given function (respiration, cardiac beating) or developmental pattern (Gu and Spitzer, 1995). In addition, to ensure function despite internal or external perturbations, these characteristics must be robust to changes in cellular or circuit parameters. The purpose of this paper is to study how the duration of the active and silent phases of episodic (i.e., periodic) activity in excitatory neural networks depend on cellular excitability and network connectivity.

Neuronal oscillators can be conceptualized as systems with fast positive feedback that leads to regenerative activity, modulated by slow negative feedback that terminates this activity, thereby allowing a new cycle to begin (Friesen and Block, 1984; Ermentrout and Chow, 2002). Here, we consider idealized, mean field models of excitatory networks (Wilson and Cowan, 1972), in which fast positive feedback is provided by the recurrent excitatory connections. Such networks can be bistable, in which case they are in either one of two states, a state of low activity and a state of high activity (Tabak et al., 2000; Wilson and Cowan, 1972). Episodic activity in this network is achieved by periodically switching between the active (high) state and the inactive (low) state, due to one or several slow negative feedback processes. We consider two types of slow negative feedback processes that act to terminate episodes in excitatory networks. The first one, synaptic depression, acts by decreasing the effective synaptic connectivity, directly reducing the amount of positive feedback in the system (a divisive effect). The second one, cellular adaptation, acts by reducing the excitability of the neurons in the network, opposing the positive feedback process (a subtractive effect).

We first analyze models that use either one of these two episode termination processes, in terms of how the duration of both the inter-episode intervals (or silent phase, SP) and the episodes (active phase, AP) are affected by network connectivity and cellular excitability. We show that despite sharing similar dynamical principles, the two models can be distinguished by the way they respond to perturbations in these two parameters (network connectivity and cell excitability). This is a generalization of results that were presented in the context of the spontaneous activity in the developing spinal cord (Tabak et al., 2000).

Because neural circuits often incorporate two or more types of feedback mechanisms, we then analyze a model that incorporates both negative feedback processes. We note that, in this multiple feedback model, the two slow processes are indirectly coupled through firing rate. We then analyze how, in this model, AP and SP are affected by network connectivity and cell excitability. Surprisingly, the model's qualitative response to variations of these parameters is not affected by the ratios of the time constants of the two slow processes. Finally, the model incorporating the two slow processes can generate episodic behavior over a much larger range of parameter values than the models incorporating either one processes.

2. Methods

We use a mean field type formulation of an excitatory network. Network activity is described by the variable a that represents the firing rate in the network (relative to the maximum network firing rate), averaged over the population and over the time scale of the synaptic dynamics (Pinto et al., 1996; Wilson and Cowan, 1972). Here, a varies between 0 (no activity in the network) to 1 (all cells fire at their highest frequency). Activity varies according to the following equation:

$$\tau_a \dot{a} = a_\infty(\tilde{s} \cdot a - \tilde{\theta}) - a \tag{1}$$

where a_∞ represents the input/output (i/o) function of the network. The sigmoid-shaped a_∞ accounts for the individual cells' i/o properties, the fast unitary synaptic conductance time course, as well as noise and heterogeneity in the network. The effective input to the network, $\tilde{s} \cdot a - \tilde{\theta}$, depends on activity because of the recurrent excitatory connections, which are the source of the positive feedback. The effective connectivity, $\tilde{s}$, and the effective average threshold, $\tilde{\theta}$ are the two key factors that can be modulated to affect network activity. Connectivity is the gain of the positive feedback loop, it encapsulates the effect of the network, while $\tilde{\theta}$ defines the set point of the network i/o, it represents the effect of cellular excitability. Figure 1 shows how the input/output function is affected by these two quantities.

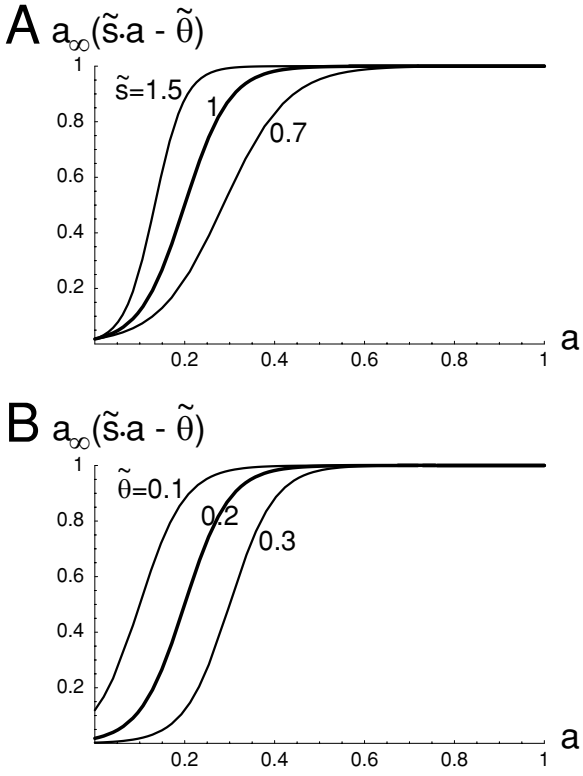

Fig. 1 The input/output (i/o) relationship of the excitatory network a_∞ can be modulated in two ways. (A) Decreasing the effective connectivity lowers the gain of the positive feedback loop (divisive effect). (B) Increasing average threshold shifts the i/o curve horizontally to the right (subtractive effect)

In our s-model, effective connectivity is slowly modulated while the cellular threshold is constant: $\tilde{s} = w \cdot s$ and $\tilde{\theta} = \theta_0$, where w is a parameter representing network connectivity, s is the synaptic depression variable, representing the fraction of available (i.e., undepressed) synapses, and θ_0 is a parameter representing the average firing threshold in the neuronal population. The s-model consists of the two equations:

$$\tau_a \dot{a} = a_\infty(w \cdot s \cdot a - \theta_0) - a \qquad (1_s)$$

$$\tau_s \dot{s} = s_\infty(a) - s \qquad (2)$$

where s_∞ is a sigmoidal function decreasing with a, so activity depresses the synapses ($s = 0$: all synapses are depressed, $s = 1$: all synapses are available). Synaptic depression decreases the gain of the fast positive feedback, a divisive effect (Fig. 1(A)).

In our θ-model, effective connectivity is constant while the effective threshold is slowly modulated by a cellular adaptation process (for example, a slow outward current). Thus, $\tilde{s} = w$ (constant) and $\tilde{\theta} = \theta_0 + \theta$ with θ representing the activation of the slow adaptation process:

$$\tau_a \dot{a} = a_\infty(w \cdot a - \theta_0 - \theta) - a \qquad (1_\theta)$$

$$\tau_\theta \dot{\theta} = \theta_\infty(a) - \theta \qquad (3)$$

with $\theta_\infty(a)$ a sigmoidal function, increasing with a, so activity renders the cells less likely to fire by increasing the effective threshold; θ can vary between 0 (no cellular adaptation) and 1 (maximal frequency adaptation). Cellular adaptation shifts the input/output function horizontally (Sanchez-Vives et al., 2000), a subtractive effect (Fig. 1(B)).

Finally, in the more general case, both synaptic depression and cellular adaptation combine to regulate episodic activity (θ-s-model):

$$\tau_a \dot{a} = a_\infty(w \cdot s \cdot a - \theta_0 - \theta) - a \qquad (1_{s\theta})$$

$$\tau_s \dot{s} = s_\infty(a) - s \qquad (2)$$

$$\tau_\theta \dot{\theta} = \theta_\infty(a) - \theta \qquad (3)$$

with the sigmoidal functions for the three models given by

$$a_\infty(v) = 1/\left(1 + e^{-v/k_a}\right)$$

$$s_\infty(a) = 1/\left(1 + e^{(a-\theta_s)/k_s}\right)$$

$$\theta_\infty(a) = 1/\left(1 + e^{-(a-\theta_\theta)/k_\theta}\right)$$

The time constants τ_s and τ_θ are very large compared to the network recruitment time constant τ_a, so we are in the relaxation limit, i.e. the transitions between high and low activity states are fast so the network is either in the low or high state. This simplifies the analysis of the models. Also, note that the two slow processes vary similarly (but in opposite ways) with a. This simplifies the analysis of the model incorporating both processes, but for slow processes with different dynamics the results described here may not apply in some situations (we have obtained similar results in a few cases for which the dynamics of s and θ were made different, but have not completed a systematic study).

Table 1 Values of the parameters used for each model, unless otherwised mentioned in text or figure

param.	s-model	θ-model	θ-s-model
w	1	1	1
θ_0	0.17	0	0
τ_a	1	1	1
k_a	0.05	0.05	0.05
τ_s	250		250
θ_s	0.3		0.3
k_s	0.05		0.05
τ_θ		250	250
θ_θ		0.3	0.3
k_θ		0.05	0.05

Simulations and analysis were done using XPPAUT (Ermentrout, 2002). Mathematica was also used to plot simulation results and phase space pictures. Commonly used values for the parameters are given in Table 1.

3. Results

3.1. Models with a single negative feedback process

The two models (s-model, using synaptic depression, and θ-model, using cellular adaptation) generate episodic activity using a common dynamical principle. In both models, a slow negative feedback variable (s or θ, depending on the model) periodically switches the network between a low and a high activity states. We now ask if the two models are affected similarly by variations of the two parameters w (network connectivity) and θ_0 (average cellular threshold in the absence of adaptation). Although this question was addressed previously in a different context (Tabak et al., 2000), the simpler models used here allow for a more complete analysis. We first show how each model responds to parameter variations, then explain these responses using phase plane analysis, and finally compare the parameter ranges that allow periodic activity for each model.

3.1.1. Effects of parameter variations on the characteristics of episodic activity

Experimentally, it is possible to manipulate both network connectivity and cellular excitability, using pharmacological

agents. Changes in both network connectivity and cellular excitability affect global network excitability. We now characterize how these changes in network excitability affect the episodic activity, specifically looking at the duration of the active and silent phases (T_{AP} and T_{SP}).

Figure 2(A) shows the effects of decreasing the connectivity, w, on the time course of activity for each model. Experimentally, this could be done by using a low dose of an excitatory neurotransmitter antagonist. When activity is regulated by synaptic depression (s-model, left panel) a decrease of connectivity leads to a slowing down of the episodic activity. This slowing down is due to an increase in the silent phase duration, as shown on Fig. 2(B), left.

If activity is instead regulated by a dynamic cellular threshold (θ-model, right panel), the same manipulation (decreasing w) speeds up the episodic activity. This faster oscillation is marked, mostly, by a decrease in the active phase duration. Thus, the two models respond differently to a reduced connectivity.

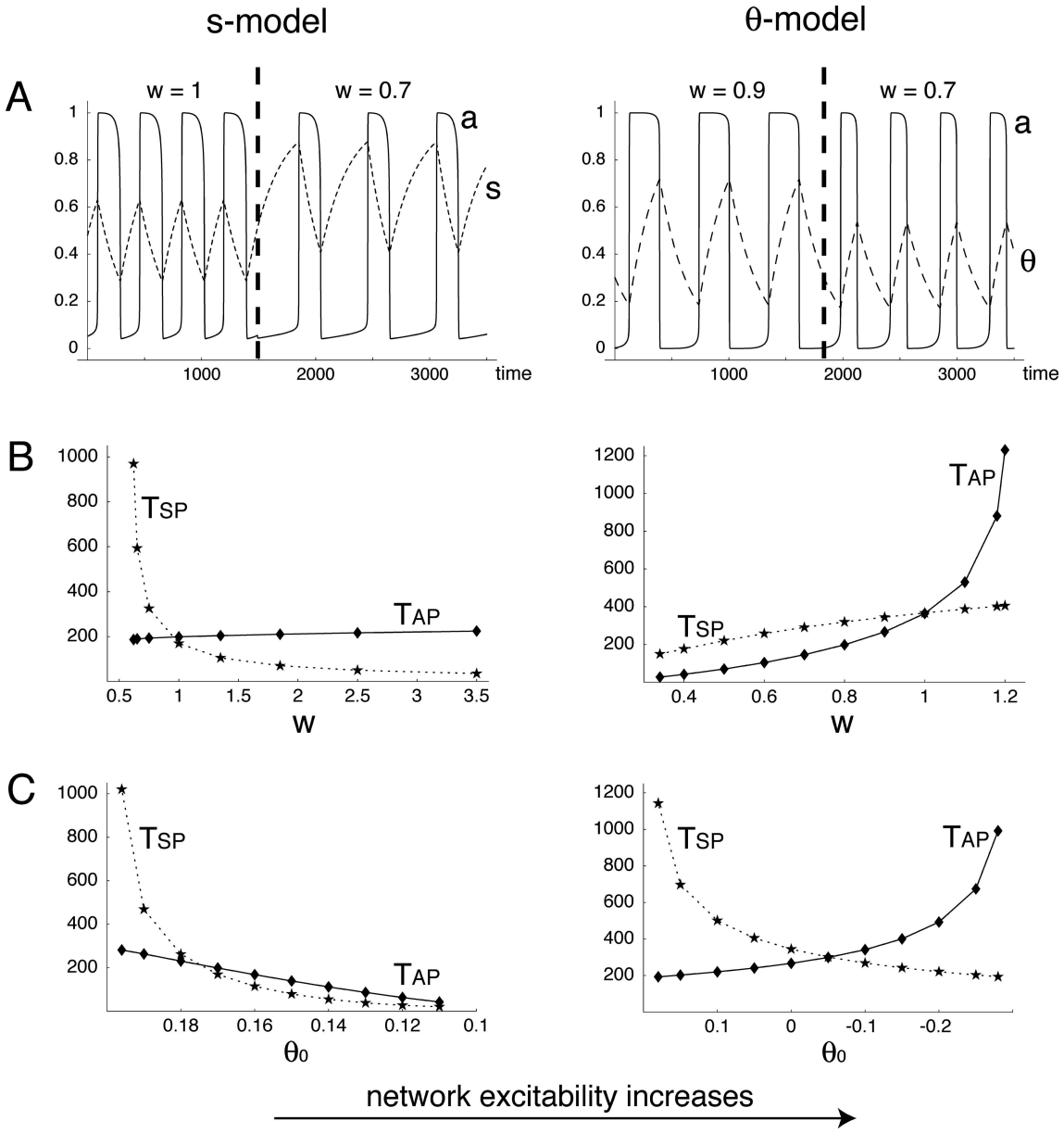

Fig. 2 Effect of changing w and θ_0 on episodic activity. (A) Time courses for activity and slow depression variable. The vertical dashed line indicates the time when w was decreased. Left, s-model, $\theta_0 = 0.17$. Right, θ-model, $\theta_0 = 0$. (B) Variations of active and silent phase durations with connectivity. Decreasing connectivity (w) leads to larger T_{SP} for the s-model (left) and shorter T_{AP} for the θ-model (right). (C) Variations of T_{AP} and T_{SP} with average cellular threshold. Left, s-model, increasing θ_0 increases T_{SP}. Right, θ-model, increasing θ_0 increases T_{SP} and decreases T_{AP}. For each panel in B, C, network excitability increases rightward

Another possible experimental manipulation is to change neuronal excitability, which is modeled here by changes of the cellular threshold θ_0. Again, the two models differ in their sensitivity to this parameter. For the s-model, increasing cellular excitability by decreasing θ_0 decreases the silent phase, (and slightly decreases the active phase, C, left panel). However, for the θ-model, decreasing θ_0 causes both T_{AP} to increase and T_{SP} to decrease (C, right panel).

To summarize, increasing network excitability (through an increase in either connectivity or cellular excitability) shortens the silent phase for the s-model, while it lengthens the active phase for the θ-model (and shortens the silent phase, in the case of a decrease in cellular threshold).

3.1.2. Phase plane analysis

These differences in response to parameter variations can be easily explained by looking at phase space diagrams (Rinzel and Ermentrout, 1998). The time courses of a and s (or θ) of Fig. 2(A) correspond to trajectories in the phase plane (a, s) (or (a, θ)). Let us first examine the left panel of Fig. 3(A). We have represented the a-nullcline (S-shaped curve, shown for 3 different values of connectivity) and the s-nullcline (dashed curve). The nullclines are the curves for which the corresponding variable has zero time derivative. The S-shaped a-nullcline represents the steady states of the excitatory network for each value of the negative feedback variable s, if s was frozen. It comprises a region of bistability (of width Δs) where the system can be in either of two stable steady states, one at high and one at low activity (there is also a middle, unstable state). However, s varies slowly, decreasing when the network is in the high activity state (active phase, ds/dt < 0 above the s-nullcline) and increasing when the network is in the low activity state (silent phase, ds/dt > 0 below the s-nullcline). The "knees" of the S-shaped a-nullcline (HK high knee, LK low knee) correspond to the transition points between active and silent phases. During each phase of the activity, the slow variable s covers the interval Δs between the two knees. The durations of the active and silent phases are determined by the horizontal position of the knees, thus in the following we focus on how the knees are affected by parameter changes.

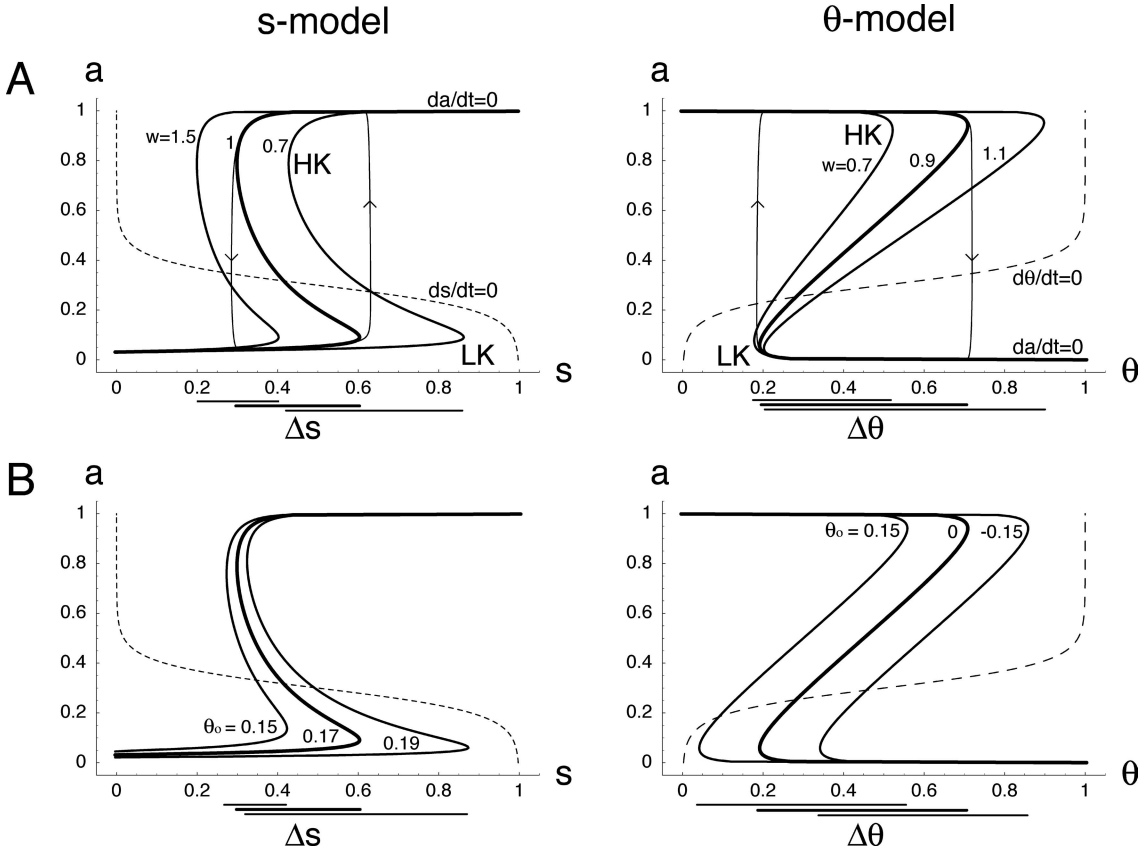

Fig. 3 Understanding the effects of parameter variations: phase plane pictures. (A) Sensitivity of the a-nullcline to w. Left, s-model, $\theta_0 = 0.17$; Right, θ-model, $\theta_0 = 0$. The trajectory coresponding to the time courses from Fig. 2(A) (left part of each panel) is represented. Transitions between high and low activity states are indicated with vertically oriented arrows. HK, high knee; LK, low knee. (B) Sensitivity of the a-nullcline to θ_0. Left, s-model, $w = 1$; Right, θ-model, $w = 0.9$. Panels A and B of this figure correspond to the cases shown in panels B and C of Fig. 2. The horizontal bars below each plot represent the bistability range (Δs, $\Delta\theta$) for each case

When the connectivity, w, is decreased, the a-nullcline is simply scaled such that the product $w \cdot s$ (the effective connectivity) is conserved at any value of a. This mostly shifts the bistability range Δs to the right (the values of s at the low/high knees, $s_{lk/hk}$, are changed by a variation in connectivity δw by a scaling factor: $\delta s_{lk/hk} = -s_{lk/hk} \cdot \delta w/w$). How does this affect the duration of the active and silent phases? At any time, s varies with a velocity proportional to $s_\infty(a) - s$, that is, the horizontal distance between the s-nullcline and the current state of the system in phase space. If the a-nullcline is moved to the right, then this distance increases for the active phase and decreases for the silent phase. Thus decreasing connectivity would decrease T_{AP} and increase T_{SP}. However, in addition to the horizontal shift to the right of the bistability range, there is also a moderate expansion of this range. This increases the distance s has to travel between each knee, increasing similarly T_{AP} and T_{SP}. The two effects (shift and expansion of Δs) add to increase T_{SP}, but they act in opposite ways on T_{AP}, so the net effect is a decrease that is small compared to the increase in T_{SP}.

The effect of a connectivity change on the θ-model is very different (Fig. 3(A) right), despite the similar dynamic nature of the oscillations in that case (the difference in shape of the a-nullcline, now Z-shaped, is simply because θ decreases during the silent phase and increases during the active phase, in opposite way to s). In this case, a change in w affects only one knee. When w is decreased, the upper knee is moved to the left (for a variation of connectivity δw, the corresponding horizontal variation of the upper knee $\delta\theta_{hk}$ can be calculated as shown in Appendix A; $\delta\theta_{hk} \simeq \delta w$) while the lower knee is almost not affected. This shortens the bistability range $\Delta\theta$, so both T_{AP} and T_{SP} are decreased. But the decreases of T_{AP} and T_{SP} are not equal. This is because the move of the higher knee to the left removes the portion of the trajectory closest (horizontally) to the θ-nullcline during AP (i.e., the slowest portion of the trajectory during AP) while it removes the portion of the trajectory furthest away from the s-nullcline during the SP (i.e., the fastest part of the trajectory during SP). Thus, T_{AP} decreases more than T_{SP} (also, the slight movement of the low knee towards the θ-nullcline tends to slow down θ during the silent phase, opposing the decrease due to the movement of the high knee; if the low knee is very close to the θ-nullcline, this effect could be strong enough that the net effect on T_{SP} is an increase).

A similar situation is shown for the sensitivity of the s-model to θ_0 (Fig. 3(B), left panel). Variations of cellular excitability affect the low knee much more than the high knee. This difference in shift between low and high knees means that the bistability range is increased with θ_0. Therefore, both T_{SP} and T_{AP} lengthen when cell excitability is decreased. However, this right shift means that the horizontal distance between the trajectory and the s-nullcline is decreased during the silent phase, further increasing T_{SP}. On the other hand, s will vary faster during the active phase, so T_{AP} increases only slightly with θ_0 compared to T_{SP}. From this case and the previous one, we see that when a parameter change affects the low (high) knee much more than the high (low) knee, T_{SP} and T_{AP} vary in the same way but T_{SP} (T_{AP}) is much more affected than T_{AP} (T_{SP}).

On the other hand, when both knees are moved in the same fashion, T_{AP} and T_{SP} vary in opposite way. This is illustrated by the last case (Fig. 3(B), right panel), where a variation of cellular threshold $\delta\theta_0$ leads to a translation $-\delta\theta_0$ of the bistability range without affecting its width. Thus, when θ_0 is increased, T_{AP} decreases and T_{SP} increases similarly.

3.1.3. Reciprocal roles of connectivity and cellular excitability

We have noted a correspondence between panels 3B left and 3A right. A variation of θ_0 causes a great variation of the low knee for the s-model. On the other hand, a variation of w causes minimal change in the low knee of the θ-model. This correspondence exists because the two models are based on the same equation for the time course of activity (Eq. (1)). The a-nullcline in each model is defined by $a = a_\infty(\tilde{s} \cdot a - \tilde{\theta})$. At a knee, if $\tilde{s}$ changes by $\delta\tilde{s}$, the corresponding variation of $\tilde{\theta}$ to keep this equation verified is $\delta\tilde{\theta} = \delta\tilde{s} \cdot a$ (as shown in Appendix A). This last equation indicates *both* the horizontal movement of a knee $\delta\tilde{\theta}$ in the θ-model due to a variation in $\tilde{s} = w$ and the movement of a knee $\delta\tilde{s}$ of the s-model due to a variation of $\tilde{\theta} = \theta_0$. In particular, at the low knee, $a \simeq 0$, so the low knee of the θ-model is almost unaffected by a change in connectivity, while the low knee of the s-model changes dramatically with a change in cellular excitability.

Thus, there is a *reciprocity* of effects of the two parameters w and θ_0 on the two slow variables θ and s. This reciprocity can be demonstrated graphically. We rewrite the nullcline equation as $a_\infty^{-1}(a) = w \cdot s \cdot a - \theta_0$ (s-model) and $a_\infty^{-1}(a) = w \cdot a - \theta - \theta_0$ (θ-model). Let us consider the θ-model. The left hand side of this last equation is shown on Fig. 4 (thick curve). If w and θ_0 are fixed, the right hand side is a straight line of slope w, which is moved vertically by changing θ. There are two particular positions of this line (i.e. two values of θ, θ_{lk} and θ_{hk}), such that it is tangent to the curve $a_\infty^{-1}(a)$, and these two positions define the low and high knees of the a-nullcline. The changes $\delta\theta_{lk}$ and $\delta\theta_{hk}$ due to a variation δw of connectivity are shown on Fig. 4. The same variation on the slope w of the tangent line entrains a much smaller variation of θ_{lk} than θ_{hk}, simply because the tangent point is much closer to the vertical axis for the low knee than for the high knee.

The same argument can be applied to changes of θ_0 when considering the s-model. On Fig. 4, replace $\delta\theta_{lk/hk}$ by $\delta\theta_0$

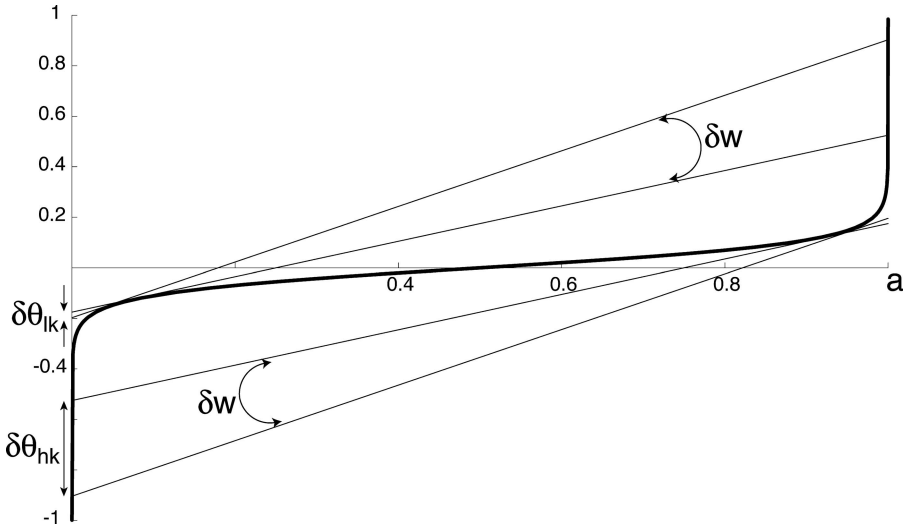

Fig. 4 Reciprocity between the effects of connectivity and cell excitability on the knees. If we consider the θ-model, the knees of the a-nullcline correspond to values a, θ verifying $a_\infty^{-1}(a) = w \cdot a - \theta - \theta_0$ such that the left and right hand sides are tangent. The thick curve corresponds to the left hand side of the equation, the thin straight lines are four examples of the right hand side that are tangent to the thick curve. If the slope of the straight line is altered by δw, the intercept of that line with the vertical axis must be changed so that the line is still tangent with the curve. For the same δw, this vertical change is much smaller for the solution corresponding to the low knee ($\delta\theta_{lk}$) than for the high knee ($\delta\theta_{hk}$). Similarly, for the s-model, a small change in the vertical intercept corresponding to the low knee would change the slope of the straight line by the same amount as a larger change of the vertical intercept corresponding to the high knee

and δw by $\delta s_{lk/hk}$. A very small variation $\delta\theta_0$ creates the same δs at the low knee that a large $\delta\theta_0$ creates at the high knee. Thus, whichever knee will change most depends on which is the parameter (w or θ_0) and which is the variable (θ or s). The pattern of knee variations shown on Fig. 3(A) right and (B) left is present because 1) both models share the same activity equation and 2) one negative feedback process has a divisive effect (i.e. controls the slope of the lines shown on Fig. 4) while the other process has a subtractive effect (i.e. controls the vertical position of the lines shown on Fig. 4).

3.1.4. Range of parameter values that supports episodic activity

We can further characterize how the horizontal position of the knees in Fig. 3 vary with parameters. Consider the θ-model ($\tilde{\theta} = \theta + \theta_0$ and $\tilde{s} = w$). We have shown that the knees' horizontal positions are altered by connectivity w (Fig. 3(A) right). We now plot the horizontal position of both knees $\tilde{\theta}_{lk/hk}$, as connectivity is varied, on Fig. 5(A). The equations of the two resulting "curves of knees" $\tilde{\theta}_{lk/hk}(\tilde{s})$ are derived in Appendix A. The trajectory showed in the (θ, a) phase space (Fig. 3(A) right) corresponds to a vertical trajectory between the two curves of knees in $(\tilde{s}, \tilde{\theta})$ space (5A). Changing connectivity simply shifts this vertical trajectory horizontally (and stretches it to fit between the two curves of knees). We first note that the two curves meet for a particular value of connectivity (w_c). If connectivity falls below this value, the knees disappear so there is no longer bistability. Second, we see that the slope of the curve corresponding to the low knee is much smaller than the slope of the high knee curve. Again, this illustrates our previous point that the low knee, in the θ-model, is very insensitive to connectivity.

From this figure, we can graphically determine the ranges of parameter values for w and θ_0 that allow periodic activity, that is, 1) the two knees exist ($w > w_c$) and 2) they correspond to values of θ between 0 and 1. Since $\tilde{\theta} = \theta + \theta_0$ oscillates between $\tilde{\theta}_{lk}(w)$ and $\tilde{\theta}_{hk}(w)$, θ oscillates between $\tilde{\theta}_{lk}(w) - \theta_0$ and $\tilde{\theta}_{hk}(w) - \theta_0$. Therefore condition 2 requires that $\theta_0 < \tilde{\theta}_{lk}(w)$ and $\theta_0 > \tilde{\theta}_{hk}(w) - 1$. These conditions define a region in parameter space (w, θ_0) which is shown on Fig. 5(B).

If we now consider the s-model ($\tilde{\theta} = \theta_0$ and $\tilde{s} = w \cdot s$), and plot the position $\tilde{s}_{lk/hk}$ of the knees as θ_0 is varied, we obtain the same curves of knees (Fig. 5(C)), since the a-nullcline and in particular the knees are defined in the same way for both models ($a = a_\infty(\tilde{s} \cdot a - \tilde{\theta})$). Note, we have kept the axes in the same directions as in panel A ($\tilde{s}$ horizontal, $\tilde{\theta}$ vertical) for comparison with panel A. So now the trajectory is horizontal, showing s vary between $\tilde{s}_{hk}$ and $\tilde{s}_{lk}$, and this trajectory shifts vertically when θ_0 is changed. Similarly to the previous case, the knees (and therefore bistability) exist only if $\theta_0 > \theta_c$. Also, since $s \leq 1$, episodic behavior requires that $w > \tilde{s}_{lk}(\theta_0)$ otherwise $\tilde{s} = w \cdot s$ can never reach the low knee $\tilde{s}_{lk}$. These two conditions are represented on Fig. 5(D).

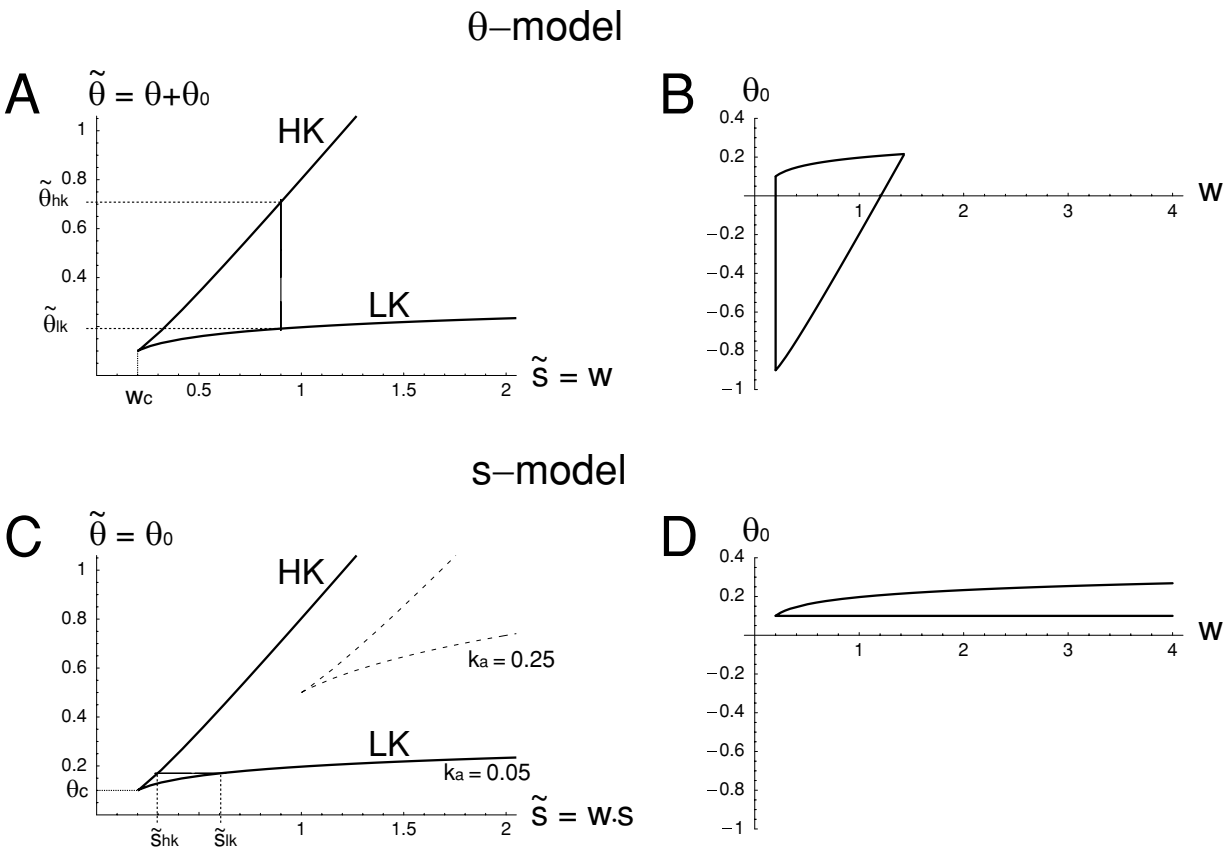

Fig. 5 Curves of knees and parameter ranges for bistability and episodic behavior. (A) Curves of knees of the excitatory network. For the θ-model, w (here 0.9) determines the range of variations of effective the threshold $[\tilde{\theta}_{lk}, \tilde{\theta}_{hk}]$. The trajectory of episodic activity is represented by a vertical lines between these two bounds. Assuming the condition for bistability is met ($w > w_c$), periodic activity can occur only if $\tilde{\theta}_{hk}(w) - 1 < \theta_0 < \tilde{\theta}_{lk}(w)$. (B) Graphical representation of these three conditions in the (w, θ_0) plane, defining the parameter region for which the θ-model can generate episodic activity. (C) Curves of knees for two values of k_a. For the s-model, θ_0 (here, 0.17) determines the position of the horizontal trajectory, with bounds $[\tilde{s}_{hk}, \tilde{s}_{lk}]$. For a given θ_0 satisfying the condition for bistability ($\theta_0 > \theta_c$), episodic activity only occurs if $w > \tilde{s}_{lk}(\theta_0)$. (D) These two conditions are represented in the (w, θ_0) plane and define a region in parameter space for which the s-model can generate episodic activity

Comparing panels B and D, we see that the θ-model can operate over a wide range of values of cellular threshold, but for a limited range of connectivity values. On the other hand, the s-model will generate episodic activity for a wide range of connectivity, but for a restricted range of cellular threshold. Thus, each model is robust to perturbations of the parameter linked to its own slow variable, since the slow variable can easily compensate a variation of that parameter. The conditions represented on panels B and D are necessary for episodic activity to occur. Whether they are sufficient depends on the dynamics of the slow variable. If the slow variable nullcline (the dashed curves in Fig. 3) intersects the a-nullcline at a point on either the high or low branch, this intersection defines a stable steady state and episodic activity does not occur. For instance, panel D shows that w has no upper limit in the case of the s-model, but for large values of w, the high knee show on Fig. 3(A) left will move to the left close to the vertical axis, and s-nullcline could intersect with the high branch of the a-nullcline. In this paper, we have used s_∞ and θ_∞ functions steep enough that these intersections would only occur if the knees horizontal position were extremely close to 0 or 1 and thus the boundaries show on Fig. 5 (B) and (D) are not significantly reduced.

Finally, we examined how the parameter k_a affected these ranges of parameter values. As shown on Fig. 5(C), increasing k_a affects the curves of knees in a way that moves the bistability range to higher values of the parameters. This is because, according to the definition of the a_∞ function (the network input/output function), multiplying k_a by a factor x is equivalent to dividing both w and θ_0 by the same factor x. Thus, to keep the same network activity, if k_a is multiplied by x, w and θ_0 must be too. For instance, the critical values of the parameters, $(w_c, \theta_c) = (4k_a, 2k_a)$ (cf. Appendix B), are increased by the same factor as k_a. Consequently, for higher k_a the excitatory network is bistable for higher connectivity and higher cellular threshold.

The consequence of this transformation for the s-model is that the range of threshold values θ_0 becomes larger. Similarly, increasing k_a leads to a larger range for w to allow episodic behavior of the θ-model.

The value k_a indicates the spread of the a_∞ function, which itself depends on the smoothness of the cellular input/output (i/o) function, and on the distribution of thresholds among the population. The steeper the cellular i/o relationship and the narrower the distribution of thresholds are, the smaller k_a will be. If the cells have steep i/o functions and there is little heterogeneity, k_a is small, thus bistability can be observed for low connectivity and high cellular excitability. However, in that case, the range of cellular threshold values allowing episodic behavior of the s-model will be very limited, i.e. the s-model will be extremely sensitive to changes in cellular excitability (cf. the large variations of the low knee with θ_0 in Fig. 3(B), left). In order for the s-model to generate robust episodic behavior (with respect to cellular excitability), it is thus necessary for the network to either have shallow cellular i/o functions, or to have a substantial degree of heterogeneity in cellular excitability.

3.2. Model with both cellular adaptation and synaptic depression

The model incorporating both cellular adaptation and synaptic depression is given by the following three equations:

$$\tau_a \dot{a} = a_\infty(w \cdot s \cdot a - \theta_0 - \theta) - a \qquad (1_{s\theta})$$

$$\tau_s \dot{s} = s_\infty(a) - s \qquad (2)$$

$$\tau_\theta \dot{\theta} = \theta_\infty(a) - \theta \qquad (3)$$

with the sigmoidal functions for the three models given by

$$a_\infty(v) = 1/\left(1 + e^{-v/k_a}\right)$$
$$s_\infty(a) = 1/\left(1 + e^{(a-\theta_s)/k_s}\right)$$
$$\theta_\infty(a) = 1/\left(1 + e^{-(a-\theta_\theta)/k_\theta}\right)$$

As in the previous models incorporating either one of the slow processes (2D models), the model with both slow processes (θ-s-model, or 3D model) switches between a low and high activity state due to the variations of both variables. During an episode, s is decreasing and θ is increasing, as shown in Fig. 6(A). However, now the phase space is three-dimensional (Fig. 6(B)), so the trajectory alternates between a high and a low state defined on a surface, the a-nullsurface (the surface of solutions to $\mathrm{d}a/\mathrm{d}t = 0$).

We can still use a two-dimensional representation by projecting the three-dimensional picture on the (s, θ) plane, as shown in Fig. 6(C). The folds of the a-nullsurface in the 3D space become the curves of knees in the 2D space. These folds of the a-nullsurface are like the knees of the a-nullcline in the previous 2D models, the transition points between the high and low states. The curves of knees are the same as in Fig. 5, since activity in the 3D model is defined exactly as in the 2D models.

However, for the 2D models, the trajectory in phase space was fully determined by the a-nullcline, assuming the slow variable nullcline intersected only on the middle branch. In other words, the dynamics of the slow variable only affected the speed at which the trajectory was followed, but not the trajectory itself. For the 3D model, the exact trajectory depends on the relative dynamics of the two slow variables, which are indirectly coupled through the fast variable a. Thus, simply looking at the nullsurface is not enough to determine the trajectory in phase space. Similarly, in the (s, θ) space, the trajectory goes back and forth between the curves of knees (Fig. 6(C)) but it is not horizontal or vertical, that is, it is not determined uniquely from the parameters w and θ_0. The location of the two points (LK, HK) on the curves of knees that are reached by the trajectory depends on the dynamics of the slow variables.

For a given value of each parameter w and θ_0, how can we determine what the trajectory will be? We approach this problem by noting that the two variables s and θ are indirectly coupled through a, so we can find a relationship between them. If we compute the average over a period of each slow variable's Eq. (2) and (3), since both derivatives' average are zero we get, after rearranging, $<s> = <s_\infty(a)>$ and $<\theta> = <\theta_\infty(a)>$ (the $<>$ notation denotes time average). Assuming that the sigmoidal functions are steep enough, during an episode $s_\infty(a) \simeq 0$ and $\theta_\infty(a) \simeq 1$ (since a is high). Similarly, during the interepisode interval $s_\infty(a) \simeq 1$ and $\theta_\infty(a) \simeq 0$. This implies that $s_\infty(a) + \theta_\infty(a) \simeq 1$ and $<\theta_\infty(a)> \simeq \%\mathrm{AP}$ (the duty cycle, i.e. $T_{\mathrm{AP}}/(T_{\mathrm{AP}} + T_{\mathrm{SP}})$. This implies in turn that:

$$<\theta> \simeq \%\mathrm{AP} \qquad (4)$$

$$<s> + <\theta> \simeq 1. \qquad (5)$$

This shows that the average of each variable is directly related to the duty cycle, and thus there is a relationship between the averages of the two variables. Using similar arguments, we can also get a relationship for the range of variation of each variable. If we define Δs and $\Delta\theta$ as the ranges covered by s and θ during episodic activity (cf. Fig. 6(C)), we can show that (cf. Appendix C)

$$\Delta s/\Delta\theta \simeq \tau_\theta/\tau_s, \qquad (6)$$

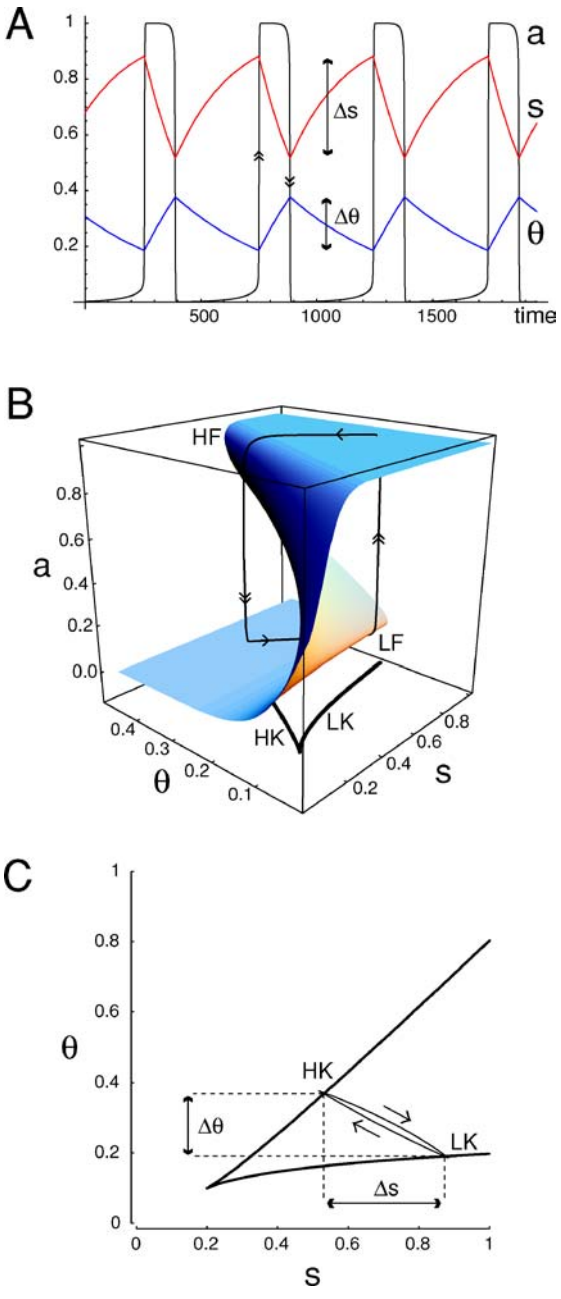

◀ **Fig. 6** Representations of the model incorporating two slow negative feedback processes, s and θ. (A) Time course of a, s and θ in the case $\tau_\theta = 2\tau_s$. $\Delta s/\Delta\theta = 1.91$, close to the ratio τ_θ/τ_s. The calculated average values of the slow variables are $<s> = 0.726$ and $<\theta> = 0.274$, close to the percent silent phase (0.729) and active phase (0.271), respectively. (B) Corresponding phase space trajectory, oscillating between high and low states of the a-nullsurface. The points for which the trajectory switches between states belong to the folds of the surface (LF, HF). Note that the lower fold is almost parallel to the s axis. The projections of the two folds on the (s, θ) plane are shown (HK, LK). The vertical double arrowheads at the transitions from low to high state correspond to the vertical double arrowheads on the time course of activity in panel A. The horizontal arrowheads on each state correspond to the arrows of the 2D trajectory on panel C. (C) Trajectory projected on the (s, θ) plane, slowly oscillating between the curves of knees . When the trajectory meets a curve of knee there is a transition between the two stable activity states (double arrowheads in A, B) and both ds/dt and $d\theta/dt$ change sign. The slope of the lower curve of knees is very small (compared to the higher curve), because the lower fold in B is almost parallel to the s axis. Note, the difference with Fig. 5 is that we used the (s, θ) plane, not the $(\tilde{s}, \tilde{\theta})$ plane, in order to see the variations of the slow variables s and θ. Therefore the "curves of knees" HK and LK will vary when the parameters w and θ_0 are changed. LF, low fold; HF, high fold; LK, curve of low knees; HK, curve of high knees

in agreement with our intuition that the faster variable necessarily covers a wider range than the slower variable in the same interval of time. This relationship between Δs and $\Delta\theta$ is also apparent on Fig. 6(A), (C) ($\tau_\theta/\tau_s = 2$, so s varies over a range twice as large as θ).

To summarize, the model incorporating both slow processes follows the same dynamical principles as the models incorporating only one slow process. However, because there is a surface—not simply a curve—of possible steady states, the system's trajectory is not predetermined by the undepressed network dynamics, it also depends on the relative timescale of the two slow processes' dynamics.

Because the two slow variables are indirectly linked through activity, there are some relationships between their average over a period and between their ranges of variation, which define the trajectory in phase space.

3.2.1. Effects of parameter variations on the characteristics of episodic activity

We now ask how the parameters w (connectivity) and θ_0 (fixed component of the firing threshold) affect the duration of the active and silent phases and how these changes compare to those described previously for the 2D models. Because the ratio of timescales of the two slow processes affects the system's trajectory in phase space, we examine three cases: $\tau_s \ll \tau_\theta$, $\tau_s = \tau_\theta$ and $\tau_s \gg \tau_\theta$.

If $\tau_s \ll \tau_\theta$, θ varies little compared to s (cf. Eq. (6)) so the full system resembles the s-model. Then, does it react to parameter variations like the s-model? Figure 7(A) and (B), left panels, shows that a decrease in connectivity leads to a decrease in both T_{AP} and T_{SP}, with a larger relative variation for T_{AP}. Thus, even though $\tau_s \ll \tau_\theta$, the θ-s-model does not react qualitatively like the s-model, but instead behaves like the θ-model (compare with Fig. 2(B)). This qualitative behavior (a reduction in connectivity decreases T_{AP}) is also obtained for the other values of the ratio τ_θ/τ_s, as shown on Fig. 7(A) and (B).

Similarly, when θ_0 is varied, the θ-s-model reacts with a change in T_{SP}, as observed for the s-model, and this behavior is also independent of τ_θ/τ_s, as shown Fig. 7(C) (compare with Fig. 2(C)). Together, these results show that for the model incorporating both slow processes, the durations of the

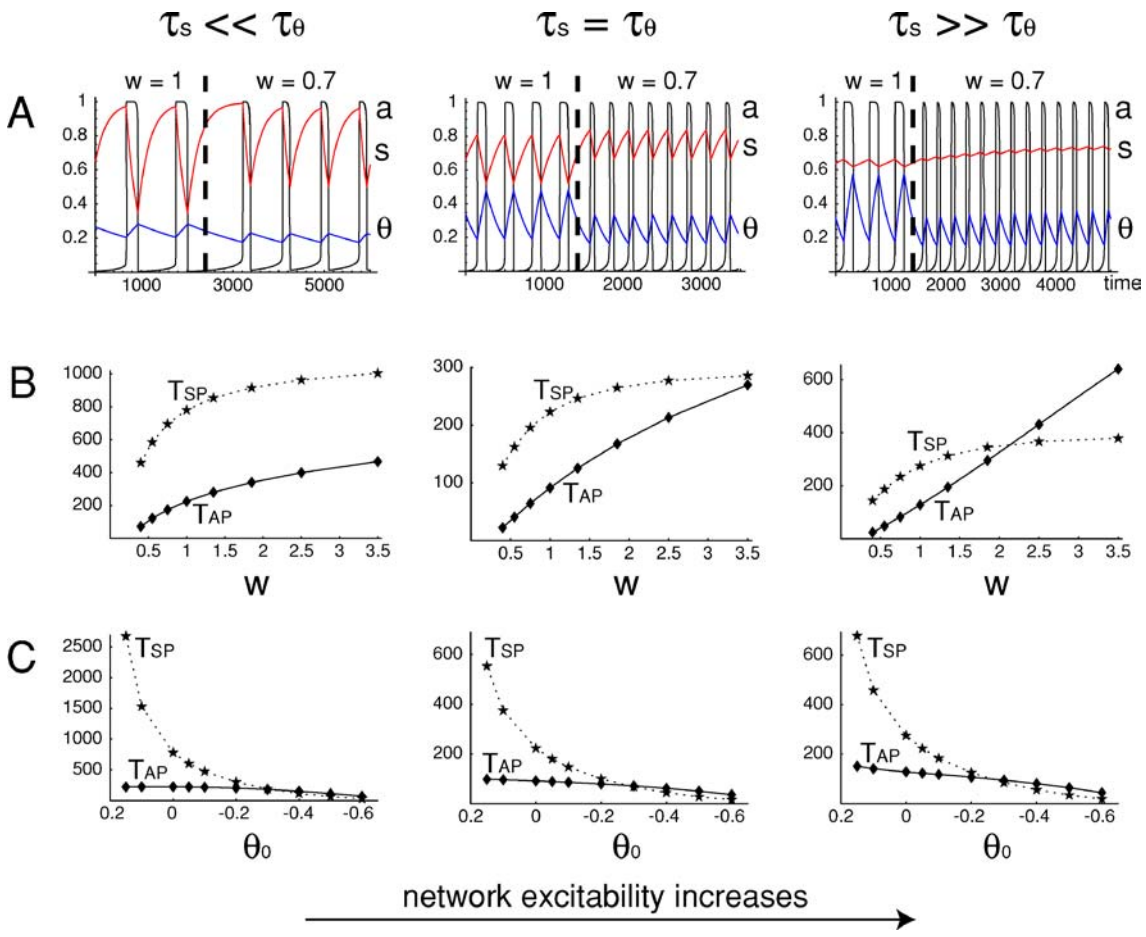

Fig. 7 Effects of parameter variations on T_{SP} and T_{AP} of the θ-s-model for various τ_θ/τ_s ratios. (A) Time courses of a, s and θ, before and after connectivity decrease. (B) Plots of T_{SP} and T_{AP} dependence on w. (C) Plots of T_{SP} and T_{AP} dependence on θ_0. Left panels: $\tau_s = 250$, $\tau_\theta = 2500$; middle panels: $\tau_s = 250$ $\tau_\theta = 250$; right panels: $\tau_s = 2500$, $\tau_\theta = 250$

active and silent phases can be set almost independently: T_{AP} *is set by connectivity*, while T_{SP} *is set by cellular excitability*.

Finally, comparing the range of parameter values on Fig. 7(B), (C) and Fig. 2(B), (C), we see that the θ-s-model is able to generate periodic activity over a similar range of w values as the s-model and over a similar range of θ_0 values as the θ-model. As the s-model and θ-model both show robustness to the parameter variation that affects their own slow process, the model incorporating the two processes shows robustness to both parameters.

3.2.2. Description of model behavior for $\tau_\theta \ll \tau_s$

For $\tau_\theta \ll \tau_s$, only θ varies significantly to terminate and initiate episodes. As shown on Fig. 7(B) and (C), right panels, varying w leads to a similar response as the θ-model, but a variation of θ_0 leads to a response resembling the s-model. Why doesn't the θ-s-model (with $\tau_\theta \ll \tau_s$) always react like the θ-model (and similarly, we could ask why the θ-s-model with $\tau_s \ll \tau_\theta$ doesn't always react like the s-model)? This is because after a parameter change the duty cycle is altered, which in turn causes the slower variable (s in the case $\tau_\theta \ll \tau_s$) to slowly vary. After a transient period, it reaches a new level (see for example Fig. 7(A), right panel: after a decrease of connectivity, s slowly increases to a new level, partly compensating the decreased w; a similar effect is shown in Bertram et al. (2000)). Thus, the net effect of a parameter change must take into account a compensatory change in the level of the slower variable. In the following, we describe the consequences of each parameter change, in the case $\tau_\theta \ll \tau_s$, using phase pictures in the (s, θ) plane.

Figure 8 shows the curves of knees and the trajectories in the (s, θ) plane for 4 combinations of values of w (varying vertically) and θ_0 (varying horizontally). Note that the curves of knees vary with these parameters. Changing the connectivity changes the slope of the high knee curve (since this slope is approximately equal to w) with little effect on the curve of low knees. On the other hand, changing cellular excitability simply shifts both curves vertically, the shift being equal to the variation of θ_0.

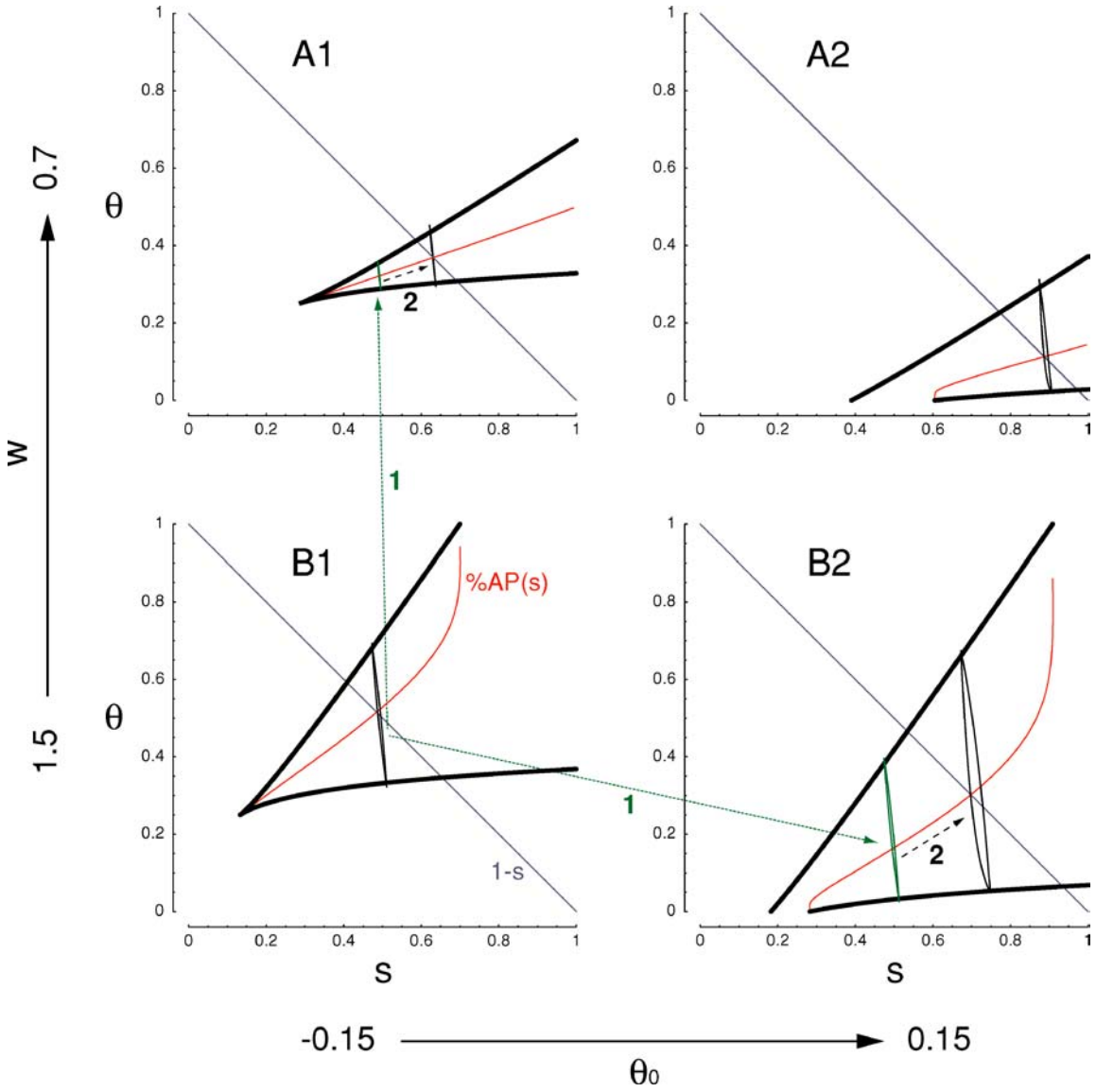

Fig. 8 Phase picture projection in the (s, θ) plane. The curves of knees are shown as well as the trajectory for various parameter combinations. From row B to A, connectivity w is decreased from 1.5 to 0.7. From columns 1 to 2, the cellular threshold θ_0 is increased from -0.15 to 0.15. To show how these two manipulations affect the trajectory, we have distinguished two steps. Decrease in connectivity (panel B1 to A1): the trajectory is first affected by the change in curves of knees (step 1, green dotted arrow to green trajectory), then settles to a new equilibrium value of s (step 2, dashed arrow). The net effect is a decrease in the length of the trajectory, mainly through a decrease of the value of θ at the end of an episode. Increase in threshold (panel B1 to B2): similarly, we show the new trajectory as if s was constant (after step 1, in green), and the final trajectory after s has equilibrated (step 2, dashed arrow). The net effect is an increase in the length of the trajectory, mostly through a decrease of the value of θ at the begining of an episode. Note, the green trajectories were not computed, they are only shown for illustration purposes. Blue lines are defined by $\theta = 1 - s$ and the red curves represent %AP(s), which depends on both w and θ_0. This is %AP for the θ-model, treating s as a parameter, calculated using an approximate formula (derived in Appendix D)

Superimposed on these plots are the projected (s, θ) trajectories (in black). Recall that during the active phase the trajectory moves from the low to the high curve of knee, during the silent phase it returns to the low curve of knee (cf. Fig. 6). Because $\tau_s \gg \tau_\theta$, the trajectories are nearly vertical, as for the θ-model. Thus, T_{AP}, T_{SP} and %AP are approximately equal to those for the θ-model with connectivity equal to $w \cdot s$ (they can be calculated, as shown in Appendix D). Before describing how the trajectory is changed by a parameter variation, we must first determine where the trajectory resides in the (θ, s) plane. Since the trajectory is almost vertical, this means finding which value of s the system has equilibrated to.

Consider the diagram shown in panel B1 ($\theta_0 = -0.15$, $w = 1.5$). We recall that there is a relationship linking the averages of the two slow variables over one period:

$<\theta> = 1 - <s> \simeq 1 - s$ since s is almost constant. The line $\theta = 1 - s$ is plotted in blue. Furthermore, we recall that $<\theta> = \%\text{AP}$ (Eq. (4)). We plotted the %AP of the θ-model as a function of s (red curve). The system operates at the value of s that meets the two conditions $<\theta> = 1 - s$ and $<\theta> = \%\text{AP}(s)$ simultaneously, thus defined by $1 - s = \%\text{AP}(s)$, that is, the intersection of the red and blue curve. Note that $\%\text{AP}(s)$ depends both on θ_0 and w and thus is different on each panel; the operating value of s (intersection of $\%\text{AP}(s)$ with the blue line) varies accordingly.

Now let us consider a decrease of connectivity. How is the trajectory affected? Because s is much slower than θ, we separate the effects of the parameter variation in two distinct steps, first keeping s constant (step 1) and then allowing it to equilibrate (step 2). The decrease of connectivity changes the curves of knees to the ones shown in panel A1. If s is constant, the trajectory simply adapts to the new curves of knees and becomes the one shown in green in A1 (step 1, represented by the green dotted arrow). The result is a reduction of the value of θ at the high knee, as we have described previously for the θ-model (Fig. 3(A) right), so active phase duration is reduced. However, this decreases the duty cycle, and therefore s will slowly increase to reach a new equilibrium, as seen on Fig. 7(A), right panel (step 2, represented by the dashed arrow). This equilibrium is defined by the intersection of the blue line and the new red curve of panel A1. Note that the shift to the right of the trajectory changes the value of θ at the high knee. This slightly counteracts the effect of the downward change in the high curve of knees (from step 1), but the net effect is still a decreased θ value at the end of the episode. On the other hand, the value of θ at the beginning of an episode has barely changed. Thus, the effect of decreasing connectivity in the θ-s-model is similar to that in the θ-model, but is less intense because s has partly compensated for this decrease.

Going back to panel B1, we now consider an increase in θ_0 that changes the curves of knees to those of panel B2. In the θ-model (s constant), this simply shifts the trajectory along with the knees, as shown in green in B2 (step 1). The effect is that θ is closer to its asymptotic value ($\theta = 0$) during the interval (going down) and further away from its asymptotic value ($\theta = 1$) during the episode (going up). Thus, T_{AP} decreases while T_{SP} increases. But again, this decreases the duty cycle, so s will slowly equilibrate to a higher value, increasing the effective connectivity (step 2). This shifts the trajectory to the right and therefore increases the value of θ at the high knee, which is back to a similar value as before the change in θ_0 (compare with panel B1). This brings T_{AP} close to its original value before changing θ_0, so the net effect (from step 1 and step 2) is mostly an increase in T_{SP}. Changing θ_0 in this model has the same effect as changing θ_0 in the s-model, mostly affecting the "low knee" (i.e., the beginning of the active phase).

We have described the effects of parameter variations in two steps: 1, immediate changes in the curves of knees due to the parameter variation and 2, slow compensatory change of the slower variable. A similar explanation can be constructed for $\tau_s \ll \tau_\theta$. Regardless of which is the slower variable, a decrease in connectivity w shortens the trajectory by moving the "high knee," affecting mostly the active phase duration; an increase in the cellular threshold θ_0 increases the length of the trajectory, mostly by moving the "low knee" end, thus predominantly affecting the silent phase. In the following section, we demonstrate that this is also the case when the two slow variables vary on the same timescale.

Finally, we note that decreasing connectivity always decreases T_{AP}, but does not always decrease T_{SP}. If cell excitability is low, that is, if θ_0 is high (above 0.1) decreasing connectivity may increase T_{SP}. This was already pointed out for the θ-model and can be understood by looking at Fig. 8 panels A2, B2. Because θ_0 is high (0.15), the low curve of knees is close to the asymptotic value of θ during the silent phase (0). When connectivity is decreased, the low curve of knees' small displacement (from B2 to A2) brings the trajectory even closer to the dashed line and this greatly slows down the recovery of θ close to 0, increasing the duration of the silent phase. In the case shown by panels B1 and A1, the low curve of knees is so far away from the lower dashed line that this effect is too small to increase T_{SP}.

3.2.3. Phase plane analysis of a reduced model for $\tau_\theta = \tau_s$

We now use a 2D reduction of the θ-s-model based on the fact that the relationship shown above between the two slow variable ($<s> + <\theta> \simeq 1$) becomes $s + \theta \simeq 1$ when $\tau_s = \tau_\theta$. As previously, we use the fact that s and θ have similar (but opposite) dynamics, i.e. $s_\infty(a) + \theta_\infty(a) \simeq 1$. Thus, adding the equations for the two slow variables (Eqs. (2) and (3)), we get $\tau_s\ (\dot{s} + \dot{\theta}) \simeq 1 - (s + \theta)$, which means that the sum $s + \theta$ approaches 1 with a time constant τ_s. Therefore, after an initial transient, $\theta = 1 - s$ so there is only one independent slow variable and we can replace θ by $1 - s$ in Eq. ($1_{s\theta}$):

$$\tau_a\, \dot{a} = a_\infty(w \cdot s \cdot a - \theta_0 - 1 + s) - a.$$

Since there is only one depressing variable, s, the phase space is two-dimensional and we can draw nullclines in this phase plane, as we did previously for the s- and θ-model.

Figure 9(A) shows how the a-nullcline is affected by changes in w. Mostly the high knee is affected. We can show that the value of s at the knees (high or low) varies with connectivity as: $\delta s_k \simeq -s_k \cdot \delta w/(w + 1/a_k)$, where a_k is the level of activity at the knee. Activity is much lower at the low knee, this is why the high knee is more affected.

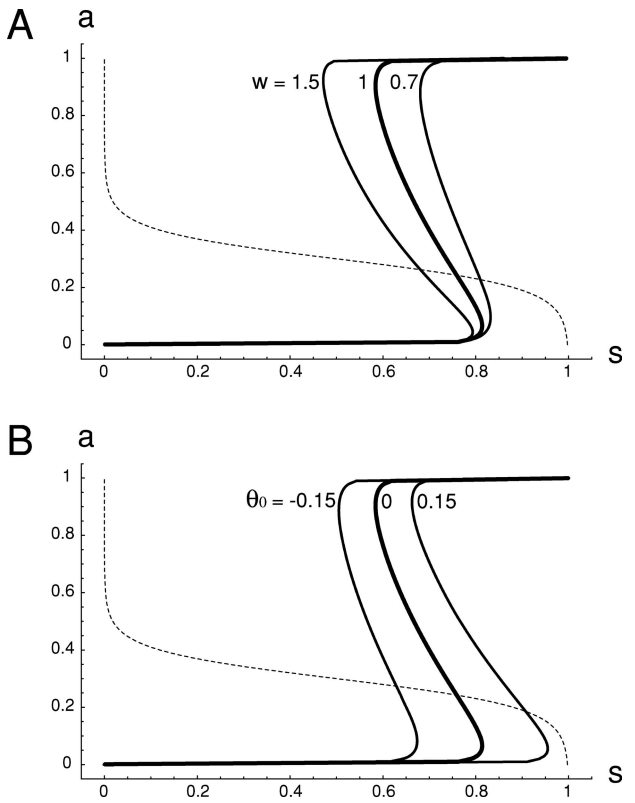

Fig. 9 Phase plane picture for the reduced model (model incorporating the two slow negative feedback processes such that $s + \theta = 1$). (A) the a-nullcline is shown for different values of connectivity. The low knee is much less affected by variations in w than the high knee. Compare to the θ-model, Fig. 3(A) right. (B) Variations of the a-nullcline with θ_0. The low knee varies more than the high knee, as with the s-model, cf. Fig. 3(B) left

Because it is mainly the high knee that varies with w, the results are similar to the θ-model (cf. Fig. 3(A), right), decreasing connectivity decreases T_{AP} (and T_{SP}, unless the low knee is very close to the s-nullcline). Since the variations in the high knee are smaller than for the θ-model, connectivity can be varied over a wider range.

In addition, since the high knee varies less with connectivity than for the θ-model, the values of w we have used are such that the high knee is still far away from the slow variable nullcline (the dashed curve), compared to the situation shown on Fig. 3(A) right. This explains why the plot of T_{AP} vs w (Fig. 7(B), middle panel) does not show the same exponential increase at high w as shown for the θ-model on Fig. 2(B) right, for the θ-model.

The changes in the a-nullcline due to changes in θ_0 are shown on Fig. 9(B). We can show that the change in the value of s at each knee δs_k can be expressed with respect to the changes in the s- and θ-model: $1/\delta s_k = (1/\delta s_k)^{s\text{-model}} + (1/\delta s_k)^{\theta\text{-model}}$. Thus, the knees vary less than for either of the 2D models. More specifically, $\delta s_k = \delta\theta_0/(1 + w \cdot a_k)$, so for the high knee the change is given by $\delta s_{hk} \simeq \delta\theta_0/(1 + w)$, while for the low knee, $\delta s_{lk} \simeq \delta\theta_0$. Thus, the low knee varies more than the high knee (by a factor $1 + w$). This picture is therefore similar to the picture for the s-model (cf. Fig. 3(B) left) and thus T_{SP} increases with θ_0. However, since the low knee does not vary as much as for the s-model, the range of θ_0 values over which episodic activity occurs is much wider than for the s-model.

3.2.4. Range of parameter values supporting episodic activity: Comparison between 2D and 3D models

We have noted above that the model incorporating the two slow negative feedback processes (reduced or not) could generate episodic activity over a wider parameter range than each of the models incorporating only one slow process. To illustrate the increase in parameter range due to having two slow processes, we plot this range in the (w, θ_0) plane (Fig. 10(A)). As for the 2D models (Fig. 5(B) and (D)), for a given connectivity (w), there is an upper and lower limit on the average cellular threshold (θ_0) for periodic activity to occur.

The upper limit on θ_0 is the same as for the θ-model (and s-model) (cf. Fig. 5(B) and (D)). If θ_0 is too high for the θ-model to generate episodes, then adding the synaptic depression variable s cannot help since s can only decrease the effective connectivity. At best $s = 1$ (the network has recovered totally from synaptic depression), so the effective connectivity is w as for the θ-model. Thus we get the same upper limit on cellular threshold $\theta_0(w)$ (corresponding to the low curve of knees) as found for the θ-model (or similarly, we could say for a given θ_0 this is the same lower limit on connectivity $w(\theta_0)$ as for the s-model).

To determine the lower limit on θ_0, we first consider the reduced $(\theta = 1 - s)$ model. The system must be bistable for episodic behavior to occur. This condition is obtained similarly to the conditions for bistability of the s-model and θ-model given above (see Appendix B), but it now involves both parameters θ_0 and w simultaneously:

$$1 + \theta_0 - \theta_c > w_c/w \tag{7}$$

(with $\theta_c = 2 \cdot k_a$ and $w_c = 4 \cdot k_a$). This second condition, together with the first, defines the range of parameter values for which the reduced model exhibits episodic activity (Fig. 10(A)).

Note that these two limits also apply to the non-reduced case, i.e. to the θ-s-model for any ratio τ_θ/τ_s. To understand these limits geometrically, we plot the curves of knees in the (s, θ) plane for a given connectivity and for two extreme values of the average cellular threshold θ_0, as well as the line $\theta = 1 - s$ (Fig. 10(B)), as in Fig. 8. The trajectory of episodic behavior, if it exists, goes from one curve of knees to the other. So in order to have episodic activity, it is necessary that the curves of knees be in the plane bounded at 0 and 1 on each axis (because both θ and s vary between 0 and 1). If θ_0

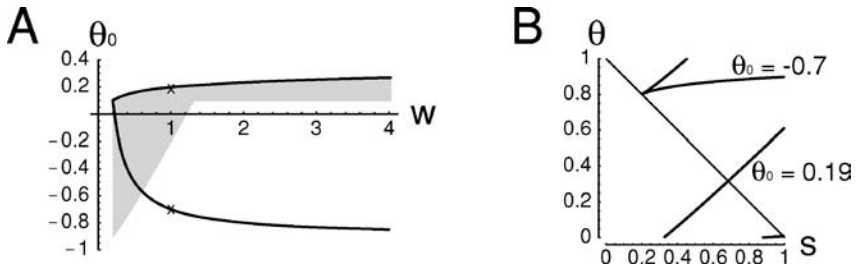

Fig. 10 Parameter range for episodic activity of the θ-s-model (reduced or not). (A) Range of parameter values allowing episodic activity. For a given connectivity w, the cellular threshold θ_0 has to be between the curves. The upper curve corresponds to the low curve of knees. The lower curve corresponds to θ_0 such that the line $\theta = 1 - s$ (panel B) intersects the curves of knees at their cusp. The two "x" symbols correspond to the cases shown in B. (B) Graphical determination of the bounds on θ_0. For $w = 1$, two sets of curves of knees are shown in the (s, θ) plane, corresponding to the lower and upper limits of θ_0 that allow episodic behavior. $\theta_0 = 0.19$: the lower curve of knees is almost entirely below the horizontal axis. For values of θ_0 above 0.19, the lower curve disappears entirely and episodic activity is lost. $\theta_0 = -0.7$: The cusp defined by the intersection of the curves of knees (coordinates $(w/w_c, \theta_c - \theta_0)$) intersects the line $\theta = 1 - s$. At this value of θ_0 or below, no trajectory can satisfy $<\theta> = 1 - <s>$, so episodic behavior is impossible

is too large ($\theta_0 \simeq 0.19$) the lower curve of knees disappears at the bottom of the plane and episodic behavior is no longer possible, the system remaining at a low steady state, unable to reach a "low knee." This defines the upper limit on θ_0. On the other hand, if θ_0 is too low ($\theta_0 \leq -0.7$) the curves of knees are above the line $\theta = 1 - s$. In this case, there is still a region of bistability with borders (the LK and HK curves) in the (s, θ) plane, but nevertheless the system cannot oscillate between the high and low state because this range of bistability is above the line $\theta = 1 - s$. Recall that the coupling between the two slow variables imply that $<\theta> = 1 - <s>$. This constraint cannot be met if the curves of knees are above the line $\theta = 1 - s$, because the point $(<s>, <\theta>)$ is always between the curves of knees (since the trajectory evolves between these two curves). It is therefore necessary that the curves of knees intersect the $\theta = 1 - s$ line, which imposes on θ_0 the lower limit given by Eq. (7).

Figure 10(A) also shows the union of the parameter ranges for the θ-model and s-model from Fig. 5(B) and (D), as a grayed area. The parameter range for the model incorporating both slow processes is greatly expanded compared to this gray area, illustrating that this model benefits from the robustness of each 2D model with respect to the parameter associated to its slow variable (w for the s-model, θ_0 for the θ-model). Notice nevertheless that part of the range of parameter values allowing episodic activity in the θ-model is excluded from the range allowing episodic behavior of the θ-s-model. This range of values does not support episodic behavior of the θ-s-model because of the indirect coupling between the two slow variables that requires $<\theta> = 1 - <s>$.

4. Discussion

We have used mean field type models of episodic behavior in excitatory networks to understand how the characteristics of episodic activity—the duration of the active and silent phases—are affected by two parameters that set the global network excitability: network connectivity (w) and average cellular threshold (θ_0). Excitatory networks are conditionally bistable. To periodically switch network activity between a high and a low state, we have considered two slow processes: one that modulates connectivity (synaptic depression) and one that modulates cellular excitability (cellular adaptation).

The model using synaptic depression (s-model) responded to a decrease in network excitability (i.e. a decrease in connectivity or an increase in cellular threshold) with a significant increase in silent phase duration (Fig. 2(B) and (C), left panels). The active phase was not affected as much as the silent phase. On the other hand, the model employing cellular adaptation (θ-model), responded to a decrease in network excitability with a significant decrease in active phase duration (Fig. 2(B) and (C), right panels). Cellular excitability, but not connectivity, could also affect significantly the silent phase duration for that model.

These sensitivities translate into limited dynamic ranges (i.e., parameter ranges over which oscillations occur). There is only modest dynamic range in the s-model for variations in cellular threshold and in the θ-model for variations in synaptic connectivity. In contrast, wide dynamic range is found in the s-model for changes in connectivity and in the θ-model for changes in cellular excitability. Such robustness derives naturally from the compensatory relationship between the parameter and the slow variable; in the s-model their product ($s \cdot w$) remains within an operating range during oscillations and in the θ-model the sum ($\theta + \theta_0$) does. In the s-model the operating range of s shifts upward as connectivity decreases and in the θ-model the operating range of theta shifts upward as cellular threshold decreases. Thus, each model shows robustness for variations in the parameter that can be compensated by the slow variable.

We then asked how the same parameter manipulations affected the active and silent phases in a model using both

Table 2 Sensitivity of each model to variations in cellular threshold and connectivity. Direction of change is indicated in parenthesis

	θ_0 (↑)	w (↓)
s-model	sensitive (T_{SP} ↑)	robust (T_{SP} ↑)
θ-model	robust (T_{SP} ↑, T_{AP} ↓)	sensitive (T_{AP} ↓)
θ-s-model	robust (T_{SP} ↑)	robust (T_{AP} ↓)

slow processes. We first reasoned that if one process was much faster than the other, the θ-s-model would react similarly to the model incorporating only the faster process. This was not the case because the slowest of the two variables would equilibrate to a new level after a parameter was varied (cf. Fig. 7(A) left and right panels), thus affecting the model's response to parameter variations. Independently of the relative speed of the two variables, a change in connectivity would affect mostly episode termination (the high knee) and thus active phase duration, as for the θ-model. On the other hand, a change in cellular threshold affected more episode onset and thus silent phase duration, as for the s-model.

Finally, because both slow variables can change their range of variations following a perturbation, the model employing both processes inherits the robustness characteristic of each slow process. Thus, the θ-s-model is robust to changes in both connectivity and cellular excitability (Fig. 10(A)).

The effects of parameter variations on all three models can be summarized as follows. If a slow synaptic depression variable (which changes the slope of the network input/output function) is present, then changing cellular excitability (θ_0, which sets the horizontal position of the network i/o function) affects the silent phase more than the active phase. Reciprocally, if a slow dynamic cellular threshold is present (θ, which changes the horizontal position of the i/o function), then changing connectivity (w, which sets the slope of the i/o function) affects the active phase more than the silent phase. The sensitivities of each model to θ_0 and w are summarized in Table 2.

4.1. Generality and extensions of the models

We have used an idealized formulation of excitatory networks, that embodies regenerative effects (fast positive feedback) via recurrent excitation. This conditionally bistable excitatory network was modulated by one or two slow negative feedback processes. One of these feedback processes, synaptic depression, modulates the excitatory feedback, a multiplicative factor in the equation defining the time course of the activity. It is said to have a divisive effect. The other process shifts the network input/output function, as an additive factor. It is said to have a subtractive effect. Generally speaking, we have thus studied a fast positive feedback system with slow divisive and/or subtractive negative feedback processes. Although we have used the terminology "synaptic depression" for the divisive process and "cellular adaptation" for the subtractive process, the actual biophysical nature of each process is not relevant to the models' behavior. This has important consequences.

First, spike frequency adaptation, a process analogous to "cellular adaptation" may change the slope of the cellular frequency/current relationship, instead of shifting its threshold point (Ermentrout, 1998). This implies that the effects of spike frequency adaptation can be modeled as divisive, not subtractive (Wilson, 2003). Thus, a cellular process (as opposed to a synaptic process) should not necessarily be modeled as a subtractive process, as we have done here for a process that dynamically affected the cellular firing threshold.

Other mechanisms can also be modeled as either divisive or subtractive processes. Shunting inhibition has a subtractive effect (Holt and Koch, 1997). On the other hand, Heeger et al. (1993) have modeled synaptic inhibition as a divisive suppression factor. A divisive effect can be obtained if inhibitory cells, activated by excitatory neurons, project back presynaptically onto axon terminals of the excitatory neurons, effectively decreasing network connectivity. This effect would be slow if the presynaptic inhibition is mediated through $GABA_B$ receptors.

Given the results presented here showing different responses to parameter variations depending on the nature of the slow negative feedback process, it is important to carefully consider whether a slow process should be modeled as subtractive or divisive.

Finally, the formalism used here for our models of network activity is qualitatively similar to the Hodgkin-Huxley (HH) formalism describing the membrane potential of excitable cells (see appendix E). Fast positive feedback in HH models is provided by fast sodium channels, the analog of excitatory neurons in our network models. Active phases in HH models are terminated by two slower processes, sodium current inactivation (divisive effect, analogous to synaptic depression here) and potassium current activation (subtractive effect, analogous to cellular adaptation here, or to activation of inhibitory neurons in other Wilson-Cowan type models). Therefore, the results presented here also apply to a class of cellular pacemakers (Results not shown, but see Tabak and Rinzel, 2005). In particular, to get bistability in cellular models, the activation function of the inward current responsible for the autocatalysis must be steep enough. For a less steep activation function, the conductance of that current must be increased, or the applied current must be decreased. Also, the relationship obtained between the two slow variables in the case of the network with two negative feedback processes translates into a relationship between the gating variables

controlling inactivation of the inward current (h) and activation of the outward current (n) in a cellular pacemaker model. This relationship, $<h> + <n> \simeq 1$, is similar to the expression commonly used to reduce the number of variables in Hodgkin-Huxley-type models of cellular excitability when h and n have similar time scales (Rinzel, 1985).

4.2. Limitations of the models

The simplicity of the present models allowed us to perform a detailed analysis of their behavior. In this subsection we discuss the various simplifications implicit in these models. Despite these simplifications our idealized models capture essential features of more complex systems.

4.2.1. Networks of spiking neurons and synaptic inhibition

Do network models constructed from populations of spiking neurons have the same properties as the mean field models described here? Obviously, the global mean field-type models cannot describe phenomenons such as wave propagation occuring in network architectures with spatially localized coupling (Butts et al., 1999; Netoff et al., 2004). We thus limit this discussion to (mostly excitatory) networks with simple topology, such that most cells in the network are activated together during the episodes. Within this limit, do our mean field models describe the mechanisms of episodic activity in networks of spiking neurons with synaptic depression or cellular adaptation?

Several studies have indeed shown that excitatory networks of leaky integrate and fire (LIF) neurons with a slow negative feedback process (either synaptic depression or cellular adaptation) can generate episodes of activity. As described here, a slow, activity-dependent negative feedback process terminates episodes by depressing network excitability and the ensuing silent phase allows the network to recover from this depression (Giugliano et al., 2004; Tsodyks et al., 2000; Wiedemann and Lüthi, 2003). However, our own work using a network of LIF neurons with synaptic depression suggests that the heterogeneity of cellular excitability allows a regime of episodic activity whereby episodes can be generated even though the undepressed network is not bistable (Vladimirski et al., submitted). This effect of heterogeneity cannot be captured with mean field models that describe the activity of one population of neurons. Nevertheless, even in this new regime of episodic activity, we found that the network responded to changes in parameters controlling connectivity and cellular excitabilitity similarly to the s-model (Vladimirski et al., submitted). Preliminary results also showed that a network of LIF neurons with cellular adaptation behaved similarly to the θ-model (J. Tabak, unpublished results).

By definition, we have considered purely excitatory networks. Whether or not our results apply to networks with inhibition will depend on the network architecture and expression mechanism of the synaptic inhibition. In many central pattern generators, for example, two sides are connected by reciprocal inhibition, allowing an alternating pattern of activity between the two sides (Marder and Calabrese, 1996). Our results do not apply to this type of network comprising two interacting populations that have distinct activities. We note, however, that some experimental and modeling studies have shown that networks with limited synaptic inhibition generate episodic activity using mechanisms similar to those described here (Compte et al., 2003; Latham et al., 2000; Staley et al., 1998; Tabak and Latham, 2003; Tsodyks et al., 2000). In these systems, inhibition probably limits network excitability, without delimiting distinct subpopulations or playing a major role in terminating the episodes.

It should also be noted that if inhibitory neurons are present in the network, synaptic depression and cellular adaptation acting on these neurons are not negative feedback processes as in the case of the purely excitatory circuits described here, but have a stimulatory effect on the excitatory population.

4.2.2. Fast oscillations during episodes

In many networks, the high state of activity during episodes may be oscillatory instead of steady (Bracci et al., 1996; Tabak et al., 2000). This fast cycling, superimposed on the slow episodes, is due to at least one additional variable, whose time scale is more like that of a. We have ignored fast cycling here, concentrating on the episodic behavior. Adding a fast synaptic depression variable to the s-model adds cycling but does not change qualitatively the behavior of the model (Tabak et al., 2000). However, we note that fast cycling may modify the response of the model to parameter variations for different model formulations (Marchetti et al., 2005).

4.2.3. Cellular oscillators

As discussed above, our mean field network model is analogous to some cellular pacemaker models. However, it must be emphasized that in the present model there are no driving force terms (i.e, it's a current based, not conductance based, formulation) and the time constants are not activity-dependent. Activity-dependent time constants would not change the trajectories of the phase diagrams of the s-model and θ-model (unless the slow time scale became too fast) and therefore would not affect the results qualitatively. However, adding different activity-dependence to the time constants for s and θ may confer new properties

to the model incorporating both processes (Smolen and Sherman, 1994). Because of their simplicity, the present models may provide a basis for more realistic models by adding other components (driving force, activity-dependent time constants, faster variables, etc.). The differences between the extended and simple models would then provide insight into the effects of the various added components.

For example, our θ-model is similar in form to the Morris-Lecar model of excitable cells. In its oscillatory regime, the period ($T_{AP} + T_{SP}$) of the Morris-Lecar model first decreases with applied current, then either plateaus or increases back to previous levels for even higher current (Skinner et al., 1993). The θ-model shows such a decrease followed by an increase (not shown, but see Fig. 2(B), right). However, in no cases did we observe a plateau of the period when θ_0 was decreased, as in the Morris-Lecar model. Thus, there are some subtle differences between the two models, which could be explored using phase plane analysis.

More biophysically detailed examples are given by Butera et al's models of cellular pacemakers in respiratory networks (Butera et al., 1999). In this work, two conductance-based models of bursting neurons (including a spike generation mechanism) were constructed. In their Model 1 (analogous to our *s*-model), bursts were terminated by the slow inactivation of a sodium channel, while their Model 2 (analogous to our θ-model) relied on the activation of a slow potassium channel. These models 1 and 2 responded like our *s*-model and θ-model to variations of applied current and maximal conductance of the inward current (Figs. 6 and 8 in Butera et al.). There was nevertheless a difference between our θ-model and their Model 2: the burst period of Model 2 would not increase for high applied current, but remained at a plateau level (like the Morris-Lecar model, cf. above). Also, Butera et al's Model 1 is very sensitive to changes in applied current (compared to their Model 2), similarly to the sensitivity of our *s*-model to θ_0 (not shown).

These examples show that although they are missing some biophysical details, our idealized models capture the behavior of more complex models of cellular oscillations.

4.3. Significance of the results

The results presented here show and explain how the duration of the active and silent phases are set by network excitability and average threshold in bursting excitatory networks, or analogously in pacemaker cells. Therefore our results may have a wide range of applications, from developing or disinhibited networks to respiratory networks, from bursting cells involved in motor patterns to cardiac pacemakers and hormone releasing cells.

4.3.1. Identification of the single (or multiple) feedback process(es)

Our present results also suggest ways to distinguish experimentally between different slow feedback processes. In the developing chick spinal cord, we have shown that decreasing excitatory connections leads to increased silent phase, without large changes in the active phase, supporting a model of episode generation based on synaptic depression, not cellular adaptation (Tabak et al., 2000). Changing the level of cellular excitability (possibly by changing the extracellular potassium concentration in *in vitro* experiments) provides a similar experimental test. Here, we also showed that in some cases it will be necessary to conduct both tests (i.e., look at changes in active and silent phases induced by both variations in connectivity and in cellular excitability), because the model incorporating both types of negative feedback can appear as one of the 2D models if only one test is conducted.

These results also apply to cellular oscillators. Consider the bursting pacemaker neurons that are involved in respiratory pattern generation, in the mammalian brainstem. Among these bursters, some are sensitive to cadmium, a calcium channel blocker, and some are sensitive to riluzole, a persistent sodium current blocker (Pena et al., 2004). Some recent results have shown that norepinephrine, thought to upregulate an inward current, had different effects on these different types of burster. Norepinephrine increased the burst duration of the cadmium-sensitive bursters, while it decreased the interburst interval of the riluzole sensitive bursters (Viemari and Ramirez, 2004). This suggests that the cadmium-sensitive bursters operate as our θ-model, i.e. using activation of a slow (calcium-activated) outward current to terminate the bursts (Model 2 of Butera et al.), while the riluzole-sensitive bursters operate as our *s*-model, using the inactivation of a persistent sodium current to terminate the bursts (Model 1 of Butera et al.). Having these two types of mechanisms may enhance the robustness of the respiratory pattern, ensuring some sort of breathing activity takes place in a variety of physiological conditions (Pena et al., 2004).

It is also crucial to identify which type of negative feedback mechanism can be involved in limiting epileptiform activities. Epileptic hippocampal networks are hyperexcitable networks that can behave like our *s*-model (Staley et al., 1998). Such networks generate bursting activity that is similar to interictal activity in epileptic patients. If one wishes to stop this interictal activity, at least two strategies are available: use drugs that decrease cell excitability, or drugs that reduce excitatory connections (or increase the strength of inhibitory connections). It is thus important to understand how active and silent phases will be affected by such pharmacological agents. We note that Yee et al. (2003)

have shown that to understand the role of anti-convulsant agents it is necessary to understand how they affect the range of variation of the slow depression process, as we have done here.

In biological systems, including neural networks, there are often not just one but several regulatory processes. The disinhibited rat spinal cord generates periodic bursts of activity on a timescale of a few seconds (Bracci et al., 1996). It is thought that these bursts are terminated by a cellular process. However, blocking this process did not abolish episodic activity, instead replacing it with slower episodes (timescale one minute), controlled by a slow type of synaptic depression (Rozzo et al., 2002). This synaptic process is much slower than the cellular process and had not been detected before blocking the cellular process. Thus synaptic depression is not thought to play a significant role in this disinhibited spinal cord preparation when the cellular process is not blocked. Our results indicate, however, that it could affect the response of the disinhibited spinal cord to variations of cellular excitability.

4.3.2. Implication for developing networks

Finally, because network activity affects network properties—particularly in the developing nervous system—understanding the dynamics of spontaneous episodic activity will be crucial in disentangling the reciprocal and interacting effects of network structure and function. Moreover, it is likely that the temporal pattern of activity is important in the regulation of cellular properties and refinement of synaptic connections (Borodinsky et al., 2004; Hanson and Landmesser, 2004; Stellwagen and Shatz, 2002). As the network matures, cellular and synaptic properties will change (in part due to the activity itself), affecting the activity pattern. We have shown previously (Tabak et al., 2000, 2001) that such episodic activity based on a synaptic depression (i.e. divisive) process was robust with respect to variations in the excitatory connectivity. Here, we also suggest that activity based on a cellular adaptation (i.e. subtractive) process would be robust to changes in cellular excitability. If both types (divisive and subtractive) of processes are involved in episodic behavior, activity will be robust to developmental changes in both synaptic transmission and cellular excitability. This robustness will be manifest in that a larger parameter range will support episodic activity and in that parameter variations will cause smaller changes in the duration of the active and silent phases. Thus, it would be advantageous for developing networks to incorporate both types of slow negative feedback processes, preventing quick changes in activity pattern to be induced by network development.

Appendix

A. Curves of knees

We consider the general equation for an excitatory network:

$$\tau_a \dot{a} = a_\infty(\tilde{s} \cdot a - \tilde{\theta}) - a. \tag{1}$$

where $\tilde{s}$ and $\tilde{\theta}$ represent the effective connectivity and effective average cellular threshold. These two quantities can be slowly (compared to a) varying in an activity-dependent way.

At steady state, $\dot{a} = 0$. This defines a surface, the a-nullsurface (shown on Fig. 6(B), its equation being written as

$$\tilde{s}(a, \tilde{\theta}) = (\tilde{\theta} - k_a \cdot \ln(1/a - 1))/a$$

or

$$\tilde{\theta}(a, \tilde{s}) = \tilde{s} \cdot a + k_a \cdot \ln(1/a - 1).$$

If one of the two quantities $\tilde{\theta}$ or $\tilde{s}$ is fixed, these become the expressions $\tilde{s}(a)$ or $\tilde{\theta}(a)$ of the a-nullcline for the s-model and the θ-model, respectively. In other words, the a-nullclines are the projection of the a-nullsurface on the planes $\tilde{\theta} = \theta_0$ or $\tilde{s} = w$. The knees of the a-nullclines correspond to the folds of the a-nullsurface. They are transition points, i.e. when the system passes a fold/knee it switches between two levels of activity. The projection of the folds on the $(\tilde{s}, \tilde{\theta})$ plane gives the curves of knees shown on Fig. 5.

To derive the equations for the curves of knees we consider the a-nullsurface $\tilde{\theta}(a, \tilde{s})$ but treat $\tilde{s}$ as a parameter. Along the folds, $\partial\tilde{\theta}/\partial a = 0$. The last equality implies that $\partial\tilde{\theta}/\partial a = \tilde{s} - k_a/(a(1-a)) = 0$. This equation gives the values of a at the knees as a function of $\tilde{s}$, $a_{lk/hk}(\tilde{s}) = 0.5(1 \mp \sqrt{1 - 4k_a/\tilde{s}})$ with the indices lk/hk meaning "low knee" / "high knee." The curves of knees, shown in Fig. 5, are then given by the equation

$$\tilde{\theta}_{lk/hk}(\tilde{s}) = \tilde{s} \cdot a_{lk/hk}(\tilde{s}) + k_a \cdot \ln(1/a_{lk/hk}(\tilde{s}) - 1). \tag{8}$$

The two curves of knee meet when $a_{lk} = a_{hk} = 0.5$, i.e. for $\tilde{s} = 4k_a$, for which $\tilde{\theta} = 0.5\,\tilde{s} = 2\,k_a$.

We can gain more insight into how $\tilde{s}$ affects $\tilde{\theta}_{lk/hk}(\tilde{s})$ by calculating $\partial\tilde{\theta}/\partial\tilde{s} = a + \partial a/\partial\tilde{s} \cdot \tilde{s} - \partial a/\partial\tilde{s} \cdot k_a/(a(a-1))$. Since at the knee $\tilde{s} - k_a/(a(1-a)) = 0$, we find that

$$\partial\tilde{\theta}_{lk/hk}(\tilde{s})/\partial\tilde{s} = a_{lk/hk}(\tilde{s}).$$

In the case of the θ-model ($\tilde{s} = w$), this expression becomes $d\theta_{lk/hk}/dw = a_{lk/hk}$ and describes how the knees

are affected by the connectivity parameter w. In general $a_{lk} \simeq 0$ and $a_{hk} \simeq 1$, we get $d\theta_{lk} \simeq 0$ (the low knee is almost unaffected by a change of connectivity) and $d\theta_{hk} \simeq dw$ (cf. Fig. 3(B), right). Similarly, for the s-model we get $ds_{lk/hk}/d\theta_0 = 1/(w \cdot a_{lk/hk})$, so the low knee varies highly with θ_0 and for the high knee $ds_{hk} \simeq d\theta_0/w$ (cf. Fig. 3(A), left).

B. Conditions for bistability

Bistability is defined by the existence of two stable states for a range of value of the slow variable of interest. The bistable zone is the zone between the two knees (between the folds for the model with two slow variables). The conditions for bistability is thus the condition for the two knees to exist. For the θ-model, the knees are defined from the nullcline equation $\theta(a)$ by $\mathrm{d}\theta/\mathrm{d}a = 0$, so $w - k_a/(a(1-a)) = 0$, as shown above. Thus, the condition for bistability is that

$$w > 4k_a.$$

If we consider the s-model, we similarly define the knees of the a-nullcline by $\mathrm{d}s/\mathrm{d}a = 0$, i.e. $1/(1-a) + \ln(1/a - 1) = \theta_0/k_a$. For a varying between 0 and 1, $1/(1-a) + \ln(1/a - 1) \geq 2$. From this, we obtain the following condition for bistability in the context of the s-model:

$$\theta_0 > 2k_a.$$

For the model incorporating both slow processes, but reduced when the two slow time constants are equal (so $\theta \simeq 1 - s$), the equation of the a-nullcline becomes: $s(a) = (1 + \theta_0 - k_a \cdot \ln(1/a - 1))/(1 + w \cdot a)$. At the knees, $\mathrm{d}s/\mathrm{d}a = 0$, implying that $(1 + w \cdot a) \cdot k_a/(a(1-a)) - w \cdot (1 + \theta_0 - k_a \cdot \ln(1/a - 1)) = 0$. This can be rewritten as $1 + \theta_0 = (k_a/w) \cdot 1/(a(1-a)) + k_a \cdot (1/(1-a) + \ln(1/a - 1))$. Since a varies between 0 and 1, $1/a(1-a) \geq 4$ and $1/(1-a) + \ln(1/a - 1) \geq 2$. Thus, θ_0 and w must satisfy:

$$1 + \theta_0 \geq w_c/w + \theta_c$$

where $w_c = 4k_a$ and $\theta_c = 2k_a$.

C. Comparison of the ranges of variation of the two variables

We now consider the model with both slow processes (θ-s-model). We sum the equations describing the variations of the two slow variables (Eqs. (2) and (3)), noting as in Results that $s_\infty(a) + \theta_\infty(a) \simeq 1$. We get $\tau_s\ \dot{s} + \tau_\theta \dot{\theta} \simeq -s - \theta + 1$. We then integrate this relationship over, say, the silent phase. We get: $\tau_s\ \Delta s - \tau_\theta\ \Delta\theta \simeq (-<s + \theta>_{SP} + 1) \cdot T_{\mathrm{SP}}$, where the notation $<>_{SP}$ indicates average over the silent phase and Δx represents the size of the range of variation of the slow variable x. Because the variations of s and θ follow a similar (mirror image) time course, the relationship obtained in Results $<s + \theta> \simeq 1$ also holds for each phase of the activity. Thus, we obtain the following relationship between the ranges of variation of the slow variables:

$$\Delta s/\Delta\theta \simeq \tau_\theta/\tau_s.$$

If s is twice as fast as θ, it will cover a range twice as large during each phase of the activity.

D. Duration of active and silent phase

Consider the θ-model. For a given w and θ_0, we can calculate $a_{lk/hk}(w)$ and the values of θ at the knees: $\theta_{lk/hk} = \tilde{\theta}_{lk/hk}(w) - \theta_0$ from Eq. (8). From these values of θ at the knees, we can derive an approximate formula for the duration of the active and silent phases, using Eq. (3) that describes the variations of θ: $\tau_\theta\ \dot{\theta} = \theta_\infty(a) - \theta$. We chose the dynamics of θ such that $\theta_\infty(a) \simeq 1$ during an episode ($a \simeq 1$) and $\theta_\infty(a) \simeq 0$ during the silent phase ($a \simeq 0$).

Thus, during the silent phase, Eq (3) becomes $\tau_\theta \cdot \dot{\theta} \simeq -\theta$. We can integrate over the silent phase and obtain $T_{\mathrm{SP}} = \tau_\theta \cdot \ln(\theta_{hk}/\theta_{lk})$. Similarly, we find $T_{\mathrm{AP}} = \tau_\theta \cdot \ln((\theta_{lk} - 1)/(\theta_{hk} - 1))$. We used these expressions to calculate $\%\mathrm{AP} = T_{\mathrm{AP}}/(T_{\mathrm{AP}} + T_{\mathrm{SP}})$ as a function of s in Fig. 8.

E. Formal analogy between network and cellular models

The activity formulation of network models with emergent oscillations used here is similar to the formulation for some cellular oscillators. We start from the equation $\tau_a\ \dot{a} = a_\infty(w \cdot a - \theta_0) - a$. Instead of considering the firing rate, a, which is a measure of the network activity (the mean firing frequency averaged over a timescale of a few spikes), we could use a measure of the (post-)synaptic drive that causes the neurons to fire, $V = w \cdot a - \theta_0$ (Pinto et al., 1996). The equation giving the variations of activity with time becomes $\tau_a \dot{V} = -V + w \cdot a_\infty(V) - \theta_0$. Here, V is the (short-time averaged) mean voltage of cells.

We note that this equation has the same form as a cellular current balance equation: $\tau_m \dot{V} = -V + \bar{g}_{in} \cdot m_\infty(V) + I_{app}$, where τ_m is the membrane time constant, $\bar{g}_{in}$ is the maximal conductance of an inward current (normalized by the leakage conductance), m_∞ is the voltage-dependent activation function of this inward current and I_{app} is the current applied to the neuron (divided by the leakage conductance). Note, the driving forces have been omitted, so it is in fact current based, not conductance based as our notation suggests. So, the analog of network connectivity w is $\bar{g}_{in}$ and the analog of the average cellular excitability of our network model is $-I_{app}$. As for the network model, the cellular model

can be bistable, and activity can be switched from the high and low states by two modulation variables: h, inactivation of the inward current, which is the analog of s, fraction of non-depressed synapses, in the network model; and n, activation of an outward current, which is the analog of θ in the network model. A cellular model with both inward current inactivation and activation of an outward current, by analogy to our network model with both synaptic depression and cellular adaptation (Eq. ($1_{s\theta}$)), would be:

$$\tau_m \dot{V} = -V + \bar{g}_{in} \cdot h \cdot m_\infty(V) + \bar{g}_{out} \cdot n + I_{app}.$$

Given the analogous formulation, the results presented here for excitatory networks are applicable to relaxation models of cellular pacemakers (h and n are slow compared to V). Note that we have not considered variations of the analog of the parameter $\bar{g}_{out}$ in this work.

References

Bertam R, Previte J, Sherman A, Kinard TA, Satin LS (2000) The phantom burster model for pancreatic β-cells. Biophys J 79: 2880–2892.

Borodinsky LN, Root CM, Cronin JA, Sann SB, Gu X, Spitzer NC (2004) Activity-dependent homeostatic specification of transmitter expression in embryonic neurons. Nature 429: 523–530.

Bracci E, Ballerini L, Nistri A (1996) Spontaneous bursts induced by pharmacological block of inhibition in lumbar motoneurons of the neonatal rat spinal cord. J Neurophysiol 75: 640–647.

Butera RJ, Rinzel J, Smith JC (1999) Models of respiratory rhythm generation in the pre-Bötzinger complex: I. Bursting pacemaker neurons. J Neurophysiol 82: 382–397.

Butts DA, Feller MB, Shatz CJ, Rokhsar DS (1999) Retinal waves are governed by collective network properties. J Neurosci 19: 3580–3593.

Compte A, Sanchez-Vives MV, McCormick DA, Wang X-J (2003) Cellular and network mechanisms of slow oscillatory activity (<1 Hz) and wave propagations in a cortical network model. J Neurophysiol 89: 2707–2725.

Coombes S, Bressloff PC (eds.) (2005) Bursting: The genesis of rhythm in the nervous system. World Scientific.

Ermentrout B (1998) Linearization of f-i curves by adaptation. Neural Comput 10: 1721–1729.

Ermentrout B (2002) Simulating, analyzing, and animating dynamical systems. SIAM.

Ermentrout G, Chow CC (2002) Modeling neural oscillations. Physiol and Behav 77: 629–633.

Friesen WO, Block GD (1984) What is a biological oscillator? Am J Physiol 246: R847–853.

Giugliano M, Darbon P, Arsiero M, Lüscher H-R, Streit J (2004) Single-neuron discharge properties and network activity in dissociated cultures of neocortex. J Neurophysiol 92: 977–996.

Gu X, Spitzer NC (1995) Distinct aspects of neuronal differentiation encoded by frequency of spontaneous Ca^{2+} transients. Nature 375: 784–787.

Hanson MG, Landmesser LT (2004) Normal patterns of spontaneous activity are required for correct motor axon guidance and the expression of specific guidance molecules. Neuron 43: 687–701.

Heeger DJ (1993) Modeling simple-cell direction selectivity with normalized, half-squared, linear operators. J Neurophysiol 70: 1885–1898.

Holt GR, Koch C (1997) Shunting inhibition does not have a divisive effect on firing rates. Neural Comput 9: 1001–1013.

Latham PE, Richmond BJ, Nelson PG, Nirenberg S (2000) Intrinsic dynamics in neuronal networks. I. Theory. J Neurophysiol 83: 808–827.

Marchetti C, Tabak J, Chub N, O'Donovan MJ, Rinzel J (2005) Modeling spontaneous activity in the developing spinal cord using activity-dependent variations of intracellular chloride. J Neurosci 25: 3601–3612.

Marder E, Calabrese R (1996) Principles of rhythmic motor pattern generation. Physiol Rev 76: 687–717.

Netoff TI, Clewley R, Arno S, Keck T, White JA (2004) Epilepsy in small-world networks. J Neurosci 24: 8075–8083.

O'Donovan MJ (1999) The origin of spontaneous activity in developing networks of the vertebrate nervous system. Curr Opin Neurobiol 9: 94–104.

Pena F, Parkis MA, Tryba AK, Ramirez J-M (2004) Differential contribution of pacemaker properties to the generation of respiratory rhythms during normoxia and hypoxia. Neuron 43: 105–117.

Pinto DJ, Brumberg JC, Simons DJ, Ermentrout GB (1996) A quantitative population model of whisker barrels: Re-examining the wilson-cowan equations. J Comput Neurosci 3: 247–264.

Rinzel J, Ermentrout GB (1998) Analysis of neural excitability and oscillations. In Methods in Neuronal Modeling. MIT Press.

Rinzel J (1985) Excitation dynamics: Insights from simplified membrane models. Fed Proc 44: 2944–2946.

Rozzo A, Ballerini L, Abbate G, Nistri A (2002) Experimental and modeling studies of novel bursts induced by blocking Na^+ pump and synaptic inhibition in the rat spinal cord. J Neurophysiol 88: 676–691.

Sanchez-Vives MV, Nowak LG, McCormick DA (2000) Cellular mechanisms of long lasting adaptation in visual cortical neurons in vitro. J Neurosci 20: 4286–4299.

Skinner FK, Turrigiano GG, Marder E (1993) Frequency and burst duration in oscillating neurons and two-cell networks. Biol Cybern 69: 375–383.

Smolen P, Sherman A (1994) Phase independent resetting in relaxation and bursting oscillators. J theor Biol 169: 339–348.

Staley KJ, Longacher M, Bains JS, Yee A (1998) Presynaptic modulation of CA3 network activity. Nature Neurosci 1: 201–209.

Stellwagen D, Shatz CJ (2002) An instructive role for retinal waves in the development of retinogeniculate connectivity. Neuron 33: 357–367.

Tabak J, Latham PE (2003) Analysis of spontaneous bursting activity in random neural networks. Neuroreport 14: 1445–1449.

Tabak J, Rinzel J, O'Donovan MJ (2001) The role of activity-dependent network depression in the expression and self-regulation of spontaneous activity in the developing spinal cord. J Neurosci 21: 8966–8978.

Tabak J, Rinzel J (2005) Bursting in excitatory neural networks. In Coombes S, Bressloff, P (eds.) Bursting: The Genesis of Rhythm in the Nervous System, World Scientific, pp. 273–301.

Tabak J, Senn W, O'Donovan MJ, Rinzel J (2000) Modeling of spontaneous activity in the developing spinal cord using activity-dependent depression in an excitatory network. J Neurosci 20: 3041–3056.

Tsodyks M, Uziel A, Markram H (2000) Synchrony generation in recurrent networks with frequency-dependent synapses. J Neurosci 20: RC50.

Viemari J-C, Ramirez J-M (2004) Role of norepinephrine in respiratory rhythm generation. Soc Neurosci Abs 755.1.

Wiedemann UA, Lüthi A (2003) Timing of network synchronization by refractory mechanisms. J Neurophysiol 90: 3902–3911.
Wilson HR, Cowan JD (1972) Excitatory and inhibitory interactions in localized populations of model neurons. Biophys J 12: 1–24.
Wilson HR (2003) Computational evidence for a rivalry hierarchy in vision. Proc Natl Acad Sci 100: 14499–14503.
Yee AS, Longacher M, Staley KJ (2003) Convulsant and anticonvulsant effects on spontaneous CA3 population bursts. J Neurophysiol 89: 427–441.